RESERVOIR WELL PERFORMANCE

AND

PREDICTING DELIVERABILITY

by

Curtis H. Whitson

Rogaland Regional College
Ullandhaug
4000 Stavanger, Norway

INTRODUCTION

Numerous publications address the subject of well performance and stabilized deliverability. Only a few, however, have received general acceptance for solving traditional production and reservoir engineering problems. Simplicity plays a significant role since the relation between rate and wellbore flowing pressure is often used by production teams only interested in approximate answers to design problems.

Productivity index, PI, is defined as the ratio of rate to pressure drop in the resevoir ($q/\Delta p$). It plays an important role in describing a well's inflow performance. PI is nearly constant for oil wells with wellbore flowing pressure above the bubble point, leading to the simplest of all inflow performance relations. Muskat[1] was one of the first to use the PI concept to understand the role of physical factors such as partial penetration, perforation density and two-phase, gas-oil flow.

The concept of skin factor, usually attributed to Hurst[2] and van Everdingen,[3] and its subsequent expression as a flow efficiency, E_F, provides a simple means to account for nonideal fluid flow. The idea can actually be found in Muskat's treatment of perforation effects on well productivity. The Hurst-van Everdingen concept of skin is a steady-state dimensionless pressure drop occuring at the wellbore. It has since been modified to account for high-velocity-flow (HVF) or turbulence effects, blockage due to the buildup of a gas or oil saturation in the near-wellbore region, and other nonideal reservoir behavior. Application of skin factor to predicting deliverability has become as important as the concept of productivity index.

An important case of oilwell inflow performance is when pressure in the reservoir sinks below the bubble point. Gas

evolves and reduces oil productivity. Evinger and Muskat[4] show that PI decreases as oil rate increases. They suggest a method to estimate the reduction in oil productivity based on steady-state flow.

The method presented by Evinger and Muskat has never been widely used. The first study on two-phase, gas-oil flow to gain acceptance by engineers came in 1968. Vogel[5] presented a simple relation between oil rate and wellbore flowing pressure based on numerical simulation of saturated-oil systems with varying rock and fluid properties. This relation has been and probably still is the industry standard for predicting oilwell performance.

The Vogel relation has been modified by several workers. Standing proposes simple extensions when a well experiences a change in flow efficiency[6] (damage or stimulation) or average reservoir pressure drops below the bubble point.[7] Patton and Goland[8] extend the Vogel relation for undersaturated reservoirs with wells experiencing drawdown below the bubble point. A recent work by Richardson and Shaw[9] proposes a generalization of the Vogel relation based on mathematical intuition. It appears from results in this study that the generalization has a physical basis.

Fetkovich[10] presents an excellent correlation of oilwell performance on data collected from over 40 multirate tests. He shows that HVF effects are present in oil wells and that absolute open flow potential (AOFP) is overestimated if such effects are not considered. He also draws the analogy between gas-and oilwell performance by comparing pressure functions which dictate the respective flow equations. It would appear that Fetkovich's study answers the request in Vogel's paper for field verification; the Vogel correlation cannot be used without first determining that HVF effects

are insignificant, and this can only be done by running a multirate test.

The present study builds on the suggestion that gas-and oilwell performance are similar and can be studied using a single approach. In particular, a dimensionless solution of the radial flow equation including HVF effects is presented in terms of the pseudopressure function. A simple correlation is given to estimate if HVF should be considered.

The oil pressure function is defined for both saturated and undersaturated oils with wellbore flowing pressures above and below the bubble point. The resulting expressions for dimensionless pseudopressure are simple to use (similar to Vogel's relation) and readily determined. It is shown that the Evinger-Muskat (EM) steady-state method of estimating oil pseudopressure is accurate enough to reproduce Vogel's results based on a numerical simulator. The EM method is simplified by the introduction of a generalized relative permeability relation. It also appears that the EM pseudopressure can be used to analyze transient well tests.

EQUATIONS AND DEFINITIONS

A general expression for the rate-pressure relation of a given phase (oil, gas, or water) is

$$q = C \cdot \int_{p_{wf}}^{p_R} F(p)dp, \quad \ldots\ldots\ldots\ldots\ldots\ldots\ldots\ldots\ldots\ldots\ldots \quad (1)$$

where q is surface rate; C is a constant composed of formation rock properties, drainage geometry, and nonideal characteristics such as partial penetration; $F(p)$ is a pressure function evaluated from wellbore flowing pressure, p_{wf}, to average reservoir pressure, p_R.

Using the pressure function suggested by Al-Hussainy, Ramey, and Crawford[11] for real gas flow, Eq. 1 can be written

$$q_g = \frac{\pi akhT_{sc}}{Tp_{sc}\{\ln(r_e/r_w)-3/4+s\}} \cdot \int_{p_{wf}}^{p_R} (2p/\mu_g Z)dp. \quad \ldots\ldots \quad (2)$$

Using the pressure function suggested by Evinger and Muskat for oil flow, Eq. 1 can be written

$$q_o = \frac{2\pi akh}{\{\ln(r_e/r_w)-3/4+s\}} \cdot \int_{p_{wf}}^{p_R} \frac{k_{ro}}{\mu_o B_o} dp. \quad \ldots\ldots\ldots\ldots \quad (3)$$

The definition of C and $F(p)$ should be obvious for Eqs. 2 and 3. kh is the permeability-thickness product; r_e/r_w is the ratio of external-to-wellbore radius, suggesting a radial drainage area; -3/4 results from the

assumption of pseudosteady-state flow, as does the use of p_R instead of initial or external boundary pressure; T is the reservoir temperature in absolute units, while T_{sc} and p_{sc} define standard conditions; s is the steady-state skin factor reflecting the composite effect of nonideal conditions; μ_g and μ_o are gas and oil viscosities; Z is the gas compressibility factor; a is a units conversion constant given in Table 1 for field and SPE preferred SI units.

The centered-well, radial-drainage assumption can be corrected by a skin factor (as suggested by M.J. Fetkovich in a personal communication) equal to $0.5 \cdot \ln(31.62/C_A)$, where C_A is the Dietz shape factor. Earlougher[12] gives values of C_A for numerous drainage shapes. By inspection it is seen that the effect of nonradial drainage boundaries is usually small: if $C_A=0.1$ (very nonradial or off-centered) then s=2.9, if $C_A=10$ (moderately nonradial) then s=0.6. The same observation is made qualitatively by Muskat.[1]

Transient Deliverability

The pseudosteady-state (pss) assumption is only valid if production time is long enough that the outer boundary has felt the effect of production. For tight, low-permeability formations or short production tests the pss assumption may need to be replaced by a transient (time-dependent) formulation. This is done by replacing p_R with initial reservoir pressure and the term $\ln(r_e/r_w)-3/4$ with an appropriate expression for dimensionless pressure.

In most situations, an expression for the transient form of $\ln(r_e/r_w)-3/4$ is the logarithmic approximation to dimensionless pressure, p_D, $(t_D>10)$:

$$\ln(r_e/r_w)-3/4 + p_D \simeq \tfrac{1}{2}\{\ln(t_D)+0.80907\}. \quad \dots\dots\dots \text{ (4a)}$$

For stimulated wells with induced-vertical-fracture half-length , x_f, an early-time expression ($t_D<0.1$) is the uniform-flux approximation:

$$\ln(r_e/r_w)-3/4 + p_D \simeq \sqrt{\pi t_D}, \quad \dots\dots\dots\dots \text{ (4b)}$$

which may apply for months or years in low-permeability reservoirs.

Dimensionless time, t_D, is given by

$$t_D = \frac{a_t k}{\phi \mu_i c_{ti} r_w^2} \cdot t. \quad \dots\dots\dots\dots\dots \text{ (5a)}$$

If the well is vertically fractured then x_f should replace r_w in Eq. 5a; also, if Eq. 4a applies, then 0.80907 should be replaced by 2.80907. Other p_D solutions can be used instead of Eqs. 4a and 4b. Earlougher gives numerous p_D solutions applying to a variety of wellbore and external-boundary geometries for large ranges of t_D.

Production time required to use the simplified pss formulation is given by

$$t_{pss} = \frac{\phi \mu_i c_{ti} A}{a_t k} \cdot t_{DApss}. \quad \dots\dots\dots\dots \text{ (5b)}$$

For most applications, t_{DApss} of 0.1 can be used; this also applies to vertically fractured wells. Values of t_{DApss} for

nonradial geometries can be found in Ref. 12. In Eqs. 5a
and 5b, ϕ is porosity; μ_i and c_{ti} are viscosity and total
compressibility at initial pressure; A is the drainage area;
k is the absolute permeability and a_t is a units conversion
factor givĎn in Table 1 for field and SPE preferred SI
units. For partially depleted reservoirs μ_i and c_{ti} should
be evaluated at average reservoir pressure.

For many reservoirs it may take from a few hours to several
weeks to reach pss conditions. In these cases the
stabilized deliverability curve can be determined from a
transient multirate test and should apply for long periods
of time. The only change in deliverability results from
changes in the pressure integral in Eq. 1.

Low-permeability (k<1md) formations may require years or
even decades to reach stabilized flow. In such cases the
concept of stabilized deliverability is no longer valid. The
constant C in Eq. 1´ changes continually and the
deliverability relation must be updated accordingly. Both
low- and moderate-permeability reservoirs may produce at a
constant wellbore or surface pressure. Once again the
concept of stabilized deliverability is not directly useful;
inflow performance is a rate-time instead of a rate-pressure
relation.

High Velocity Flow (Turbulence)

The effect of turbulence or high velocity flow (HVF) is
not included in Eqs. 1 to 3. It is commonly accepted that
gas flow can be influenced by HVF. This effect is usually
expressed as a rate-dependent skin, Dq_g. Fetkovich gives
conclusive evidence that HVF also exists in saturated and
undersaturated oil systems. Field data suggest that HVF can
dominate the oil-rate equation and that rate-dependent skin

is equally applicable. Based on these observations the following developments were made to generalize the analysis of multirate gas- and oilwell tests, including prediction of stabilized deliverability.

First, an equation was developed to estimate the minimum rate, q_{HVF}, at which HVF effects might be expected,

$$q_{HVF} = a_{HVF} \frac{r_w h_p \mu}{\gamma}, \quad \dots \dots \dots \dots \dots \dots \dots \dots \dots \dots \quad (6)$$

where r_w is the wellbore radius; h_p is the perforated producing thickness; μ is gas or oil viscosity at the minimum-expected wellbore flowing pressure; γ is specific gravity of gas or oil at standard conditions, relative to air or water, respectively; a_{HVF} is a units conversion factor given in Table 1 for field and SPE preferred SI units. Eq. 6 is derived by assuming a Reynold's number of one at the onset of HVF, and an average grain diameter of 0.5mm.[1,10] The assumptions were made intentionally to give a pessimistic estimate of q_{HVF}.

For saturated-oil reservoirs, q_{HVF} for gas should be compared with gas rate calculated from $q_o(R-R_s)$ where q_o is the maximum oil rate expected during stabilized production, R is the producing gas-oil ratio (GOR) and R_s is the solution GOR at the minimum-expected wellbore flowing pressure. A multirate test should be run if either gas or oil q_{HVF} is lower than the maximum gas or oil rate expected during stabilized production.

Rewriting Eq. 1 and including rate-dependent skin, Dq, gives

$$q = C \frac{\ln(r_e/r_w)-3/4+s}{\ln(r_e/r_w)-3/4+s+Dq} \cdot \int_{p_{wf}}^{p_R} F(p)dp. \quad \ldots\ldots\ldots\ldots \quad (7)$$

The following definitions are made to simplify the following development:

$$m(p) = \int_{p_a}^{p} F(p)dp, \quad \ldots\ldots\ldots\ldots\ldots\ldots\ldots\ldots\ldots\ldots \quad (8a)$$

$$m_d = 1 - m(p_{wf})/m(p_R), \quad \ldots\ldots\ldots\ldots\ldots\ldots \quad (8b)$$

$$Q_{max} = C \cdot m(p_R), \quad \ldots\ldots\ldots\ldots\ldots\ldots\ldots\ldots\ldots \quad (8c)$$

$$q_d = q/Q_{max}, \quad \ldots\ldots\ldots\ldots\ldots\ldots\ldots\ldots\ldots\ldots \quad (8d)$$

$$D_d = \frac{Q_{max}}{\ln(r_e/r_w)-3/4+s} D. \quad \ldots\ldots\ldots\ldots\ldots\ldots \quad (8e)$$

The definition of pseudopressure function, $m(p)$, uses atmospheric reference pressure (the lower integration limit) according to the definition of AOFP. m_d is a dimensionless form of the pseudopressure drop which equals q/Q_{max} if $D=0$. Q_{max} is a theoretical (no-HVF) AOFP, whereas the true AOFP, q_{max}, may only be a small fraction of Q_{max} if HVF effects are significant. The definition of dimensionless

rate-dependent-skin term, D_d, results from the previous definitions.

Solving Eq. 7 in terms of dimensionless parameters gives

$$D_d \cdot q_d^2 + q_d - m_d = 0, \dots\dots\dots\dots\dots\dots\dots\dots\dots \text{(9)}$$

or

$$q_d = \frac{1 + (1 + 4 \cdot D_d \cdot m_d)^{0.5}}{2 \cdot D_d} \; ; \; D_D \neq 0, \dots\dots\dots\dots \text{(10a)}$$

$$q_d = m_d \; ; \; D_d = 0. \dots\dots\dots\dots\dots\dots\dots\dots\dots \text{(10b)}$$

Fig. 1 presents the solutions of Eq. 9 graphically for several values of D_d. This log-log type curve has proven useful for analyzing multirate test data and predicting stabilized deliverability.

PRESSURE FUNCTIONS

The pressure function, $F(p)$, in Eq. 1 is defined differently for gas and oil systems. The gas function only considers pressure effects caused by fluid properties; note that $p/\mu_g Z$ is directly porportional to $1/\mu_g B_g$. The oil function includes the pressure dependence of oil relative permeability, implying two-phase gas-oil flow. Gas condensate reservoirs also exhibit two-phase gas-oil flow. They are not considered here because of insufficient understanding and estimation of their PVT properties.

Gas Reservoirs

Calculation of the pseudopressure function can be simplified by making certain assumptions about the behavior of the pressure function.[13] F(p) for gases can be separated into three regions as shown in Fig. 2. The <u>low-pressure region</u> (<10000 kPa or 1500 psia) can be approximated by a straight line with zero intercept, yielding:

$$F(p) = 2 \cdot \left(\frac{1}{\mu_g z}\right)_{p*} \cdot p, \dots\dots\dots\dots\dots\dots\dots \text{(11a)}$$

and

$$m_d = 1 - (p_{wf}/p_R)^2, \dots\dots\dots\dots\dots\dots \text{(11b)}$$

where p* is any low pressure in the linear region. Eqs. 11 can actually be used in any pressure region if the drawdown is small enough and p* is taken as the average of p_R and p_{wf}. Unfortunately this latter case is seldom found in practice and it should not be used unless the assumptions on which it is based are fully understood.

At high pressures (>22500 kPa or 3500 psia) the gas $F(p)$ function is nearly constant and the following simplification results:

$$F(p) = 2 \cdot (\frac{p}{\mu_g Z})_{p*} \simeq \text{constant}, \quad \ldots\ldots\ldots\ldots\ldots \quad (12a)$$

and

$$m_d = 1 - (p_{wf}/p_R), \quad \ldots\ldots\ldots\ldots\ldots\ldots \quad (12b)$$

where $p*$ is any pressure in the region where $F(p)$ is constant, though the value at p_R is often used. This case corresponds to a constant productivity index. The problem with using Eqs. 12 is that wellbore flowing and average reservoir pressure must always remain in the high-pressure region where $F(p)$ is constant.

As the search for gas reservoirs goes deeper and to lower-permeability formations, the range p_R to p_{wf} often stretches over all three pressure regions, thus making both the low- and high-pressure assumptions invalid. In general the integral form of $m(p)$ given in Eq. 2 should be solved numerically, graphically or analytically. The resulting $m(p)$ function is valid for both wellbore flowing and average reservoir pressures during the entire production life of a gas well.[11]

Oil Reservoirs: Simplified Approach

Fetkovich suggests that $F(p)$ for oil systems can be approximated by two straight lines joined at the bubble point. This is shown schematically in Figs. 3. Above the bubble point, $F(p)$ only reflects the pressure dependence of oil viscosity and formation volume factor. Defining y as the ratio of $F(p_R)$ to $F(p_b)$, then

$$y = \frac{(\mu_o B_o)_{p_b}}{(\mu_o B_o)_{p_R}}. \quad \dots \dots \dots \dots \dots \dots \dots \dots \dots \dots \dots \quad (13)$$

for $p_R \geq p_b$.

Defining x as the ratio of $F(p_a)$ (i.e., at atmospheric pressure) to $F(p_b)$, then

$$x = \frac{(k_{ro}/\mu_o B_o)_{p_a}}{(k_{ro}/\mu_o B_o)_{p_b}}. \quad \dots \dots \dots \dots \dots \dots \dots \dots \dots \quad (14)$$

for $p_R \geq p_b$.

For undersaturated reservoirs there are two cases to consider, as shown in Figs. 3a and 3b. Case I corresponds to a completely undersaturated reservoir where $p_b \leq p_{wf} \leq p_R$. Case II corresponds to an undersaturated reservoir with wells producing at flowing pressures below the bubble point, or $p_{wf} \leq p_b \leq p_R$. For both cases the $F(p)$ function is given by

$$F(p \geq p_b) = F_b + \frac{(1-y)F_b}{(p_b - p_R)} \cdot (p - p_b) \quad \dots\dots\dots\dots\dots \quad (15a)$$

and

$$F(p \leq p_b) = x \cdot F_b + \frac{(1-x)F_b}{p_b} \cdot p. \quad \dots\dots\dots\dots\dots \quad (15b)$$

Fig. 3c shows Case III for a saturated oil reservoir at or below its bubble point. Generalizing the definition of x as the ratio of $F(p_a)$ to $F(p_R)$ at $p_R \leq p_b$, and assuming it remains constant at all stages of depletion, the general form of the saturated-pressure function is

$$F(p \leq p_b) = x \cdot F_R + \frac{(1-x)F_R}{p_R} \cdot p. \quad \dots\dots\dots\dots\dots \quad (16)$$

Using the linear relations suggested by Eqs. 15 and 16, the following three expressions for dimensionless pseudopressure, m_d, result:

$p_b \leq p_{wf} \leq p_R$: Completely Undersaturated

$$m_d = 2 \cdot v \cdot y \cdot (p_R/p_b - p_{wf}/p_b)$$

$$+ \frac{v \cdot (1-y)}{(p_R/p_b - 1)} \cdot (p_R/p_b - p_{wf}/p_b)^2, \quad \ldots\ldots\ldots\ldots \quad (17)$$

$p_{wf} \leq p_b \leq p_R$: Undersaturated; Saturated Flowing Pressure

$$m_d = 1 - 2 \cdot v \cdot x \cdot (p_{wf}/p_b) - v \cdot (1-x) \cdot (p_{wf}/p_b)^2, \quad \ldots\ldots \quad (18)$$

where

$$v = \frac{1}{(x+1) + (y+1)(p_R/p_b - 1)}; \quad \ldots\ldots\ldots\ldots\ldots \quad (19)$$

$p_{wf} \leq p_R \leq p_b$: Completely Saturated

$$m_d = 1 - V(p_{wf}/p_R) - (1-V)(p_{wf}/p_R)^2, \quad \ldots\ldots\ldots\ldots \quad (20)$$

where

$$V = \frac{2 \cdot x}{(x+1)}. \quad \ldots\ldots\ldots\ldots\ldots\ldots\ldots\ldots\ldots\ldots\ldots \quad (21)$$

It was found that the minimum value of y for physically realistic systems ranges from 1.0 to 0.885 for p_R/p_b of 1.0 to 2.0, as shown in Fig. 4a. The effect of y on m_d (i.e., q_o/q_{omax} if D=0) is negligible, as shown in Fig. 4c. If y is set to one, then approximate expressions can be written for Eqs. 17, 18 and 19,

$p_b \leq p_{wf} \leq p_R$: Completely Undersaturated

$$m_d = 2 \cdot v \cdot (p_R/p_b - p_{wf}/p_b), \quad \dots \dots \dots \dots \dots \dots \quad (22)$$

$p_{wf} \leq p_b \leq p_R$: Undersaturated; Saturated Flowing Pressure

$$m_d = 1 - 2 \cdot v \cdot x \cdot (p_{wf}/p_b) - v \cdot (1-x) \cdot (p_{wf}/p_b)^2, \quad \dots \quad (23)$$

where

$$v = \frac{1}{(x+1)+2(p_R/p_b-1)}; \quad \dots \dots \dots \dots \dots \dots \quad (24)$$

The general quadratic relation for saturated oils, Eqs. 20 and 21, can probably be used for both undersaturated and saturated conditions. The resulting simplicity should usually outweigh any loss in accuracy. The dashed curves in the lower half of Fig. 4c illustrate the potential error in using Eqs. 20 and 21. Fig. 5a shows the saturated-oil pressure function, relative to its value at average reservoir pressure, corresponding to various values of V in Eq. 20.

It cannot be overemphasized that if HVF effects are neglible ($D \approx 0$) then $m_d = q/q_{max}$. For example, the simplest relation, as suggested by **Fetkovich**, assumes the pressure function has zero intercept ($x=0; V=0$), resulting in

$$q/q_{max} = 1 - (p_{wf}/p_R)^2, \quad \dots \dots \dots \dots \dots \dots \quad (25)$$

which can be compared with **Vogel's relation** ($x=1/9; V=0.2$),

$$q/q_{max} = 1 - 0.2(p_{wf}/p_R) - 0.8(p_{wf}/p_R)^2. \ \ldots\ldots\ldots \ (26)$$

Actually, Eq. 20 is a special case of Eq. 18 when $p_R/p_b=1$. The same quadratic form is given by Richardson and Shaw (see Fig. 5b). They suggest the equation as an intuitive generalization of Vogel's relation (V=0.2, D=0) for saturated reservoirs. Vogel's results actually show a variation in V from 0.1 to 0.7. It appears that V remains constant during most of depletion and increases after recoveries of 8 to 10% initial oil in place. Vogel's average value of V=0.2 corresponds to early depletion.

Physically, V of 0.2 for saturated reservoirs corresponds to a linear F(p) function with intercept equal to one-nineth the value at average reservoir pressure (see Fig. 5a). The value of $F(p_R)$ changes according to conditions dictated by the material balance, as shown schematically in Fig. 3c.

For all field examples given by Fetkovich (except Field A, which is a highly depleted, low-pressure reservoir), maximum drawdown is 20% or less. It can be shown that independent of the pressure function used, backpressure slope n appears the same at low drawdowns, though extrapolated AOFP's differ. Using delta-pressure-squared versus rate corresponds to assuming x of zero (V=0), which results in a relatively pessimistic AOFP. The error in AOFP and stabalized deliverability may vary, depending on the nature of the true pressure function. If HVF effects are not present (D=0) then the error caused by using the delta-pressure-squared plotting technique can be expressed as $-100 \cdot x/(1+x)$ percent.

Fig. 6 shows a Fetkovich example plotted as oil rate versus $1-(p_{wf}/p_R)^2$, corresponding to x of 0.0 or V of 0.0, and oil

rate versus $1-0.4(p_{wf}/p_R)-0.6(p_{wf}/p_R)^2$, corresponding to x of 0.25 or V of 0.4. Backpressure slope, n, is the same for both curves ($\approx$ 0.62), but AOFP's are 795 and 890 Sm^3/d (5000 and 5600 STB/D), respectively. The insert figure shows pressure functions corresponding to the two definitions of m_d. Fetkovich gives an analogous example (his Fig. 22) showing that delta-pressure (V=1, x=1) versus rate yields an AOFP of 5406 Sm^3/d (34000 STB/D), whereas using delta-pressure-squared (V=0,x=0) versus rate yields an AOFP of 1526 Sm^3/d (9600 STB/D); backpressure slopes of both plots are the same (n=0.81).

Oil Reservoirs: Evinger-Muskat Method

Evinger and Muskat suggest a method for calculating the m(p) function from PVT and relative permeability data. It assumes that producing GOR is constant at all points in the reservoir. This method is probably the most rigorous available without access to a simulator. It is shown in this study that Vogel's results, based on a numerical model, can be reproduced using the steady-state method of Evinger and Muskat (see Fig. 7).

First, PVT properties (R_s, B_o, μ_o, B_g and μ_g) are tabulated from initial to atmospheric pressure (see Table 2). The producing GOR, R, is specified. At each tabulated pressure the gas-oil relative permeability ratio, k_{rg}/k_{ro}, is calculated from the relation

$$k_{rg}/k_{ro}(p) = \{R - R_s(p)\} \frac{\mu_g(p)B_g(p)}{\mu_o(p)B_o(p)} \quad \ldots\ldots\ldots\ldots (27)$$

If experimental relative permeability data are available, k_{rg}/k_{ro} should be plotted directly versus k_{ro}, as shown in Fig. 8. If experimental data are not available, then one of the curves in Fig. 8 can be used. Pore size distribution factor of one should be used for most reservoirs; ten applies to unconsolidated sandstones and one-half to highly consolidated sandstones.

Having calculated $k_{rg}/k_{ro}(p)$ from Eq. 27, $k_{ro}(p)$ is found from the relative permeability relation. The pressure function $k_{ro}/\mu_o B_o$ is tabulated and plotted versus pressure. The m(p) function can be calculated numerically as follows. First, $F(p) \cdot \Delta p$ is calculated at p_k, where $F(p)$ is the average of values evaluated at pressures p_k and p_j, and $\Delta p = p_k - p_j$. The m(p) function is calculated by summing the

$F(p) \cdot \Delta p$ values, starting at atmospheric pressure. The calculation procedure is shown in Table 2.

Dimensionless pseudopressure, m_d, can be calculated and plotted versus p/p_R as shown in Fig. 7. The best-fit value of V for Vogel's results is 0.2. The Evinger-Muskat method usually reproduces simulated results with good accuracy.

The EM method also can be applied to analysis of transient well tests. Although this application is not rigorous it appears to be accurate enough for practical puposes.

Raghavan[14] suggests separate drawdown and buildup pseudopressure functions. The calculation procedure for each is essentially the same as proposed by Evinger and Muskat. At a given drawdown time and wellbore flowing pressure, producing GOR is used to calculate k_{rg}/k_{ro} (Eq. 27), and therefrom k_{ro}, $k_{ro}/\mu_o B_o$ and $m(p_{wf})$. Producing GOR at shut-in is assumed to apply throughout the buildup period.

Boe, et al.[15] show that after very short times the producing GOR becomes constant during transient testing. In practice this means that observed GOR is constant during a drawdown test and can be used to calculate both drawdown and buildup $m(p)$ functions. This method was used to analyze drawdown and buildup tests given by Raghavan, resulting in estimated permeabilities of 6.19 and 6.45 md, respectively; model permeability of 6.16 md is reported by Raghavan. Producing GOR's used by the EM method in each case were 69.10 Sm^3/Sm^3 (388 scf/STB) and 333.2 Sm^3/Sm^3 (1871 scf/STB), respectively.

Boe, et al.'s drawdown and buildup tests were also analyzed using the EM method with R of 267.2 Sm^3/Sm^3 (1500 scf/STB). Estimated permeabilities were 11.8 (short DD), 12.3

(BU; short DD) and 10.6 (BU; long DD). Model permeability reported by Boe, et al. is 10 md. Although the estimated permeabilities are only approximate, they are a considerable improvement over using pressure only.

One problem with using the EM method is when producing GOR is less than R_s at a given drawdown or buildup pressure. Eq. 22 gives negative k_{rg}/k_{ro} for this situation, which also can arise using the Raghavan buildup method; Raghavan does not address the problem. Based on limited results in this study it appears that bubble-point GOR can be used instead of producing GOR if $R < R_{sb}$. In practice this situation only arises at early stages of depletion before critical gas saturation has been reached throughout the drainage radius of the well.

ANALYZING MULTIRATE TEST DATA

A general procedure is suggested for analyzing multirate test data for gas and oil reservoirs. The dimensionless log-log type curve is used to determine HVF effects and predict deliverability. If only a single-rate well test is available, then the same procedure is followed without type-curve matching; a value of D_d is assumed (e.g. zero) or estimated from a correlation.

Procedure

1. Organize and tabulate available rock and fluid data for the particular well.

2. Determine the pseudopressure function.

· For gas reservoirs m(p) is defined by PVT data — namely μ_g and Z. First plot $p/\mu_g Z$ versus pressure, then

integrate using atmospheric base pressure. Numerical integration using the trapezoid rule is often simple and accurate (Table 3 gives an example of the procedure).

• For oil reservoirs the EM method can be used to estimate $m(p)$. Assuming $R=R_{sb}$, k_{rg}/k_{ro}, k_{ro}, $k_{ro}/\mu_o B_o$, and $m(p)$ are calculated. For undersaturated reservoirs the process is continued at $p>p_b$ holding k_{ro} at its initial (gas-free) oil value. For partially depleted reservoirs R may be considerably greater than R_{sb} and the EM procedure can be repeated. The results can then be simplified by plotting m_d versus p/p_R and fitting the data to one of the curves in Fig. 4. The best-fit value of V is then used with the generalized m_d relation (Eq. 21).

Using the straight-line pressure function for saturated oils, $m(p)$ need only be calculated at average reservoir pressure. The necessary relations are:

$$m(p) = \left(\frac{k_{ro}}{\mu_o B_o}\right)_{PR} \cdot \int_0^p \left\{x + \frac{(1-x)p}{p_R}\right\}dp \quad \dots\dots\dots (28a)$$

or

$$m(p) = \left(\frac{k_{ro}}{\mu_o B_o}\right)_{PR} \cdot \left\{x \cdot p + \frac{(1-x) \cdot p^2}{2p_R}\right\}. \quad \dots\dots\dots (28b)$$

If V is assumed, then x equals $V/(2-V)$. Based on Vogel's results, V is 0.2 and x is 1/9, resulting in

$$m(p) = \frac{1}{9} \cdot \left(\frac{k_{ro}}{\mu_o B_o}\right)_{p_R} \cdot \left(p + \frac{4}{p_R} \cdot p^2\right) \quad \ldots\ldots\ldots\ldots\ldots \quad (29a)$$

Assuming x=0 and V=0, as suggested by Fetkovich, results in a simpler relation which is recommended for practical applications,

$$m(p) = \frac{1}{2p_R} \cdot \left(\frac{k_{ro}}{\mu_o B_o}\right)_{p_R} \cdot p^2 \quad \ldots\ldots\ldots\ldots\ldots\ldots \quad (29b)$$

For undersaturated oils, first calculate $m(p_b)$ using Eq. 28 or 29 and $p_R = p_b$. $m(p)$ at undersaturated pressures is calculated from

$$m(p) = m(p_b) + \frac{1}{2} \cdot (1+y)(p-p_b) \cdot \left(\frac{k_{ro}}{\mu_o B_o}\right)_{p_b} \cdot \quad \ldots\ldots\ldots\ldots \quad (30)$$

3. Note $m(p_R)$.

4. Convert each wellbore flowing pressure to a dimensionless pseudopressure m_d.

5. Plot m_d versus rate on tracing paper, using the grid of Fig. 1.

6. Match the data with one of the D_d type curves by adjusting the tracing paper from left to right, making sure that axes are held parallel to the type curve. Only one degree of freedom is allowed in the matching process. This should ensure a unique match.

7. Note the match point: q_M, q_{dM} and D_d.

8. Calculate the theoretical maximum AOFP, $Q_{max} = q_M/q_{dM}$. True AOFP, q_{max}, is read from the matched type curve at m_d of 1.

9. Assuming permeability is known, calculate the term $\ln(r_e/r_w)-3/4+s$. For gas wells,

$$\{\ln(r_e/r_w)-3/4+s\} = \frac{\pi akhm(p_R)}{Q_{max}} \cdot \frac{T_{sc}}{T \cdot p_{sc}}, \quad \dots\dots\dots (31a)$$

and for oil wells,

$$\{\ln(r_e/r_w)-3/4+s\} = \frac{2\pi akhm(p_R)}{Q_{max}} \quad \dots\dots\dots\dots (31b)$$

10. Calculate D from $\{\ln(r_e/r_w)-3/4+s\} \cdot D_d/Q_{max}$.

11. Determine if flow periods are stabilized - i.e., if pss has been reached. If wellbore flowing pressure versus time plots as a straight line on cartesian coordinates, then flow is probably stabilized during production. When pressure-time data are not available, Eq. 5b can be used to estimate if production time is greater than t_{pss}.

12a. If t_{pss} is reached during flow periods then the rate-m_d curve traced from the type curve is the stabilized deliverability curve. The term $\ln(r_e/r_w)-3/4$ should be estimated from drainage area, though a value near eight should usually suffice.

12b. If t_{pss} is not reached during flow periods then the term $\ln(r_e/r_w)-3/4$ should be estimated from a p_D function, e.g., Eq. 4a or 4b.

13. Calculate skin by subtracting $\ln(r_e/r_w)-3/4$ found in Step 12, from $\ln(r_e/r_w-3/4+s$, found in Step 9.

14. If a change in skin is anticipated, say from a stimulation treatment, then the test deliverability can be shifted to reflect the change in skin. This is done by calculating a new AOFP as

$$q_{max,new} = q_{max,test} \cdot \frac{\{\ln(r_e/r_w)-3/4+s\}_{test}}{\{\ln(r_e/r_w)-3/4+s\}_{new}} \ \ldots \ (32)$$

The new value is located on the tracing paper at m_d of 1; this point is aligned with the type curve found from the test-data match and a new deliverability curve is drawn.

The same procedure is followed for low-permeability reservoirs having a transient rate solution. $\ln(r_e/r_w)-3/4$, or more correctly, p_D, can be calculated at several times (e.g., 1, 2, 5, and 10 years) and deliverability curves drawn for each time based on corrected q_{max} (Eq. 32).

Appendix A discusses the method suggested by Standing for correcting the rate equation in saturated-oil reservoirs which are damaged (HVF effects are neglected by Standing).

15. For saturated-oil reservoirs a similar correction must be made because of depletion. Material balance results can be used to estimate $k_{ro}/\mu_o B_o$ at several points of depletion. The procedure is to correct the true AOFP and shift the deliverability curve using the following relation:

$$q_{max,new} = q_{max,test} \cdot \frac{(k_{ro}/\mu_o B_o)_{PR,new}}{(k_{ro}/\mu_o B_o)_{PR,test}} \cdot \frac{p_{R,new}}{p_{R,test}} \quad (33)$$

This simplified correction for depletion is the same as proposed by Standing[7] using the Vogel pressure function. It is also suggested by Fetkovich.

An alternative method is to calculate the EM $m(p)$ function at each new producing GOR. The engineer must decide if the extra calculations are justified for predicting future deliverability.

EXAMPLE 1: SIMULATED GASWELL MODIFIED ISOCHRONAL TEST (MIT)

The first example considers a low-permeability gas reservoir with rock and fluid properties given in Table 3. A numerical model including turbulence effects was used to simulate the test procedure given in Table 4. The model was checked against numerous published results.

Data from the 24-hour buildup are analyzed in Fig. 9. Calculated permeability (0.009 md) is about 10% lower than model permeability. Calculated skin (0.87) is about 33% lower than calculated by subtracting $p_D(t_D)$ (Eq. 4a) from calculated m_D at $p_{wf,s}$. Deviations result from the relatively short production period (12 hours); transient effects do not reach far into the reservoir, and turbulence dominates the small drainage region. Since similar errors might be expected in actual tests of low-permeability reservoirs, the calculated k and s are used to analyze MIT results.

MIT data given in Table 4 are analysed using the previously proposed procedure. Starting with step 3, results are as follow:

3. $m(p_R)$ is equal to $m(p_i)$ or $2.973 \cdot 10^7$ $kPa^2/Pa \cdot s$. For MIT, however, the correct $m(p_R)$ to use for calculating m_d (Step 4) is $m(p)$ corresponding to p_{ws} immediately before the drawdown begins. For rates 565.2, 1130.5, 1695.7, and 2261.0 Sm^3/d, $m(p_R)$ are $2.965 \cdot 10^7$, $2.935 \cdot 10^7$, $2.889 \cdot 10^7$, and $2.834 \cdot 10^7$ $kPa^2/Pa \cdot s$, respectively.

4. Table 4 gives m_d for each wellbore flowing pressure.

5. Fig. 10 shows the type-curve match of q_g-m_d data using Fig. 1.

6. The D_d=2 type curve is chosen to give a best-fit.

7. The match point is chosen as q_{gM}=6218 Sm^3/d at q_{DM}=1.

8. The theoretical AOFP is 6218 Sm^3/d. True AOFP of 3109 Sm^3/d is read from Fig. 10 at m_d of 1.

9. Using calculated permeability (0.009 md) and Eq. 29a, $\ln(r_e/r_w)$-3/4+s is 2.833.

10. D is $2.833 \times 2/6218$ or $9.11 \cdot 10^{-4}$ $1/Sm^3/d$. Using the model value for HVF factor, β, D is $1.06 \cdot 10^{-3}$ $1/Sm^3/d$, a reasonable check. Although skin resulting from HVF effects at 3109 Sm^3/d is only 3, it reduces AOFP to half its theoretical (no-HVF) value.

11. Production after 8 hours is not stabilized, as is easily shown by calculating t_D of $6.20 \cdot 10^{-5} \cdot t(hr)$, or t_D (t=8hr) of $4.96 \cdot 10^{-4}$. To reach pss after only 8 hours would require a drainage radius of 6.71 m, clearly smaller than the true drainage area.

12b. The term $\ln(r_e/r_w)$-3/4 is replaced by $p_D(t_D)$ given by Eq. 4a, and equals 3.230.

13. Steady-state skin is 2.833-3.230 or -0.4, which should be compared with zero used in the model. Practically, the

value of -0.4 would be interpreted as zero since no
stimulation has been used.

14. This gas well is an obvious candidate for acid- or
hydraulic-fracture treatment. Assuming a vertical
fracture of 76.2 m half-length can be created, the following
analysis is performed.

After stimulation, test deliverability will shift to the
right in Fig. 10. Using Eq. 32, the true AOFP at 1, 2, 5,
10, and 25 years is calculated and given in Table 5. Fig. 10
shows the shifted deliverability curves; note that the
original test curve is reached after 25 years.

If the well produces at constant wellhead pressure, then a
tubing performance curve can be imposed on Fig. 10. This
would yield rate as a function of time, the relation needed
for engineering design.

EXAMPLE 2: SATURATED OILWELL ISOCHRONAL TEST

The basic data for this example are taken from
Fetkovich's Well 5-C, Field D. PVT and relative
permeability data were estimated from correlations (Table
6). Measured rates and pressures at the end of each 4-hour
drawdown are given in Table 7. Six months separate the two
four-point tests and average reservoir pressure has dropped
about 690 kPa.

Pseudopressures are calculated using the EM method assuming
R equal to the bubble-point solution GOR. $m(p_i)$ equals
19.63 kPa/Pa·s. After depletion of 690 kPa, $k_{ro}/\mu_o B_o$ at
average reservoir pressure of 24821 kPa is 90% its initial
value. Using the producing GOR calculated by a Tarner
material balance (Table 6), pseudopressures are

recalculated. $m(p_R)$ is 97% $m(p_i)$, considerably less change than $k_{ro}/\mu_o B_o$ experiences. This suggests a potential error using the correction procedure given by Eq. 30. The following analysis uses $m(p)$ calculated by the EM method at producing GOR.

The test data are analyzed using the multirate procedure presented earlier. Starting with Step 3, results are as follow:

3. $m(p_i)$ is 19.63 kPa/Pa·s. At p_R of 24821 kPa, $m(p_R)$ is 19.07 kPa/Pa·s.

4. Wellbore flowing pressures are converted to m_d in Table 7.

5. Fig. 11 shows the type-curve match of q_o-m_d with Fig. 1.

6. The D_d=20 type curve is chosen to give a best-fit. Flows A-3 and B-1 appear to deviate from the other data.

7. The match point is q_{oM} of 7631 Sm^3/d at q_{DM} of 1.

8. Theoretical AOFP is 7631 Sm^3/d. True AOFP is 1526 Sm^3/d, as read from Fig. 11 at m_d of 1.

9. Using permeability reported by Fetkovich from buildup analysis and core data (2470 md), $\ln(r_e/r_w)$-3/4+s is 20.4 using Eq. 31b. $m(p_R)$ of 28 kPa/Pa·s is assumed.

10. D is 20.4x20/7631 or 0.0535 1/Sm^3/d.

11. Time to pseudosteady-state flow, t_{pss}, based on a drainage area of 2.59·10^6 m^2 (640 acres) is approximately six hours.

12a. The term $\ln(r_e/r_w)-3/4$ is replaced by $p_D(t_D)$. Using Eq. 4a, its value is 8.7.

13. Steady-state skin is 20.4-8.7 or 11.7.

14. If steady-state skin calculated in Step 13 is due to damage (well is fully penetrating), then an acid treatment should clean up the near-wellbore region. Assuming skin can be reduced to zero, the change in deliverability is estimated by correcting the true AOFP and shifting the deliverability curve. Also, $\ln(r_e/r_w)-3/4$ at stabilized conditions should replace $p_D(t_{D4hr})$. For 640-acre spacing, the value of $\ln(r_e/r_w)-3/4+s$ is 8.35 with s=0. Stabilized AOFP is 1526x20.4/8.35 or 3729 Sm^3/d. The deliverability curve is shown in Fig. 11.

The above procedure was repeated using the delta-pressure-squared procedure suggested by Fetkovich. Results are presented in Table 7 and Fig. 11 (dashed lines).

CONCLUSIONS

The purpose of this paper has been to review well-known aspects of predicting reservoir well performance and to present some new concepts which have been developed. Perhaps the most important point to be made is that gas- and oilwell tests should be conducted and analyzed in the same manner. The study gives a description of nonideal behavior of gas and oil flow; in particular, high velocity flow (turbulence) and variation in the pressure function have been described. Several conclusions are made based on the results of this study:

1. A dimensionless solution of the radial flow equation has been developed. It accounts for rate-dependent effects,

steady-state skin, and variation in the pressure function. The solution is equally applicable to gas and oil wells.

2. The Vogel inflow performance relation has been given physical meaning. It represents an expression of the radial flow equation based on the following two assumptions: (a) no high-velocity-flow effects are present (D=0), and (b) the saturated-oil pressure function, $k_{ro}/\mu_o B_o$, is a linear function with intercept at atmospheric pressure having one-nineth the value at average reservoir pressure.

3. General expressions for dimensionless pseudopressure of oil wells are developed based on the straight-line pressure functions suggested by Fetkovich. These expressions, equal to Vogel's dimensionless rate, q_o/q_{omax}, if rate-dependent effects are negligible, are applicable to undersaturated- and saturated-oil reservoirs producing at wellbore flowing pressures above and below the bubble point.

4. A good approximation of dimensionless pseudopressure for oil wells producing at saturated or undersaturated reservoir pressures is the original Vogel expression for dimensionless rate. The possible error introduced by using the Vogel relation is no larger than reported by Vogel for saturated systems having different PVT and relative permeability relations than the reservoir used to develop his general correlation.

5. The Evinger-Muskat method for predicting oilwell performance at saturated conditions is reviewed. The method is made easier-to-use by introducing generalized relative permeability curves.

6. It is shown that the Evinger-Muskat method for calculating oil pseudopressure is applicable to transient well test analysis. Saturated-oil drawdown and buildup

tests reported in the literature were used to check the validity of the method.

7. A general procedure is given for analyzing multirate tests performed on gas and oil wells. Two examples illustrate the procedure.

8. Standing's method for correcting the Vogel relation for damaged and stimulated wells is discussed. The assumptions on which it is based are given, and improvements are suggested. It appears that the original method is physically unrealistic for wells with negative skin.

NOMENCLATURE

a = units-conversion constant in flow equation

a_{HVF} = units-conversion constant in high-velocity-flow equation

a_t = units-conversion constant in dimensionless-time equations

A = area, m^2 (ft^2)

B = formation volume factor, m^3/Sm^3 (ft^3/scf or RB/STB for gas or oil, respectively)

c_{ti} = initial (or average reservoir pressure) total compressibility, kPa^{-1} (psi^{-1})

C = constant in flow equation

D = high-velocity-flow term, $1/Sm^3/d$ ($1/scf/d$)

D_d = dimensionless high-velocity-flow term

E_F = flow efficiency

$F(p)$ = pressure function (also F; $F_b = F(p_b)$, etc.), $kPa^2/Pa \cdot s$ or $kPa/Pa \cdot s$ ($psia^2/cp$ or $psia/cp$) for gas or oil, respectively

h = total formation thickness, m (ft)

h_p = perforated or producing thickness, m (ft)

k = absolute permeability, μm^2 ($md \simeq \mu m^2$)

k_{rg} = relative permeability to gas

k_{ro} = relative permeability to oil

m = semi-log slope of Horner plot, $kPa^2/Pa \cdot s/cycle$ or $kPa/Pa \cdot s/cycle$ ($psia^2/cp/cycle$ or $psia/cp/cycle$) for gas or oil, respectively

$m(p)$ = pseudopressure function, $kPa^2/Pa \cdot s$ or $Kpa/Pa \cdot s$ ($psia^2/cp$ or $psia/cp$) for gas or oil, respectively

m_d = dimensionless pseudopressure function

n = reciprocal of slope of log-log rate-pseudopressure (backpressure) curve

p = absolute pressure, kpa (psia)

$p*$ = specific pressure in low- or high-pressure region

of gas reservoirs, kPa (psia)

p_a = atmospheric pressure, kPa (psia)

p_b = bubble-point pressure, kPa (psia)

p_D = dimensionless pressure

p_R = average reservoir pressure, kPa (psia)

p_{sc} = pressure at standard conditions, kPa (psia)

p_{skin} = average pressure in the skin region, kPa (psia)

p_{wf} = measured wellbore flowing pressure, kPa (psia)

$p_{wf,s}$ = wellbore flowing pressure at shut-in, kPa (psia)

Δp_s = pressure drop due to skin in near-wellbore region, kPa (psia)

q_d = dimensionless rate = q/Q_{max}

q_g = surface gas rate, Sm³/d (scf/D)

q_{HVF} = surface rate at the onset of high velocity flow (turbulence), Sm³/d (scf/D or STB/D for gas or oil, respectively)

q_{max} = <u>true</u> maximum surface rate (AOFP), Sm³/d (scf/D or STB/D for gas or oil, respectively)

Q_{max} = <u>theoretical</u> maximum surface rate (AOFP) if a well had no HFV effects, Sm³/d (scf/D or STB/D for gas or oil, respectively)

r_e = external-boundary drainage radius, m (ft)

r_w = wellbore radius, m (ft)

R = producing gas-oil ratio, Sm³/Sm³ (scf/stb)

R_s = solution gas-oil ratio, Sm³/Sm³ (scf/stb)

s = steady-state skin factor

S = saturation, fraction

t = time, hours unless otherwise specified

t_D = dimensionless time

t_{pss} = time to reach pseudosteady state, hours

t_{DApss} = dimensionless time to reach pseudosteady state

T = absolute temperature, K (°R)

T_{sc} = absolute temperature at standard conditions, K (°R)

V = parameter in general quadratic rate equation

x = ratio of pressure function $F(p)$ at atmospheric pressure to $F(p)$ at average reservoir pressure (<u>saturated-oil</u> reservoirs); ratio of pressure function $F(p)$ at atmospheric pressure to $F(p)$ at bubble-point pressure (<u>undersaturated-oil</u> reservoirs)

x_F = vertical-fracture half-length, m (ft)

y = ratio of pressure function $F(p)$ at average reservoir pressure to $F(p)$ at bubble-point pressure for <u>undersaturated</u> reservoirs

Z = real-gas compressibility factor

Greek Symbols

μ = viscosity, Pa·s (cp)

ϕ = porosity, fraction

Subscripts

g = gas

new = evaluated at new reservoir conditions

o = oil

test = evaluated at test conditions

Superscripts

$E_F=1$ = value of property (q or p_{wf}) which would be measured if steady-state skin was zero (flow efficiency equal to one)

$E_F \neq 1$ = rate which would be measured if steady-state skin was nonzero (flow efficiency different than one)

REFERENCES

1. Muskat, M.: Physical Principles of Oil Production, International Human Resources Development Corporation, Boston(1981).

2. Hurst, W. "Establishment of the Skin Effect and Its Impediment to Fluid Flow Into a Wellbore," Pet.Eng. (Oct.,1953) Vol. 25,B-6.

3. van Everdingen, A.F.: "The Skin Effect and Its Influence on the Productive Capacity of a Well," Trans., AIME (1953), Vol. 198, 171-176.

4. Evinger, H.H. and Muskat, M.: "Calculation of Theoretical Productivity Factor," Trans., AIME (1942) Vol. 146, 126-139.

5. Vogel, J.V.: "Inflow Performance Relationships for Solution-Gas Drive Wells," J.Pet.Tech. (Jan., 1968) 83-92.

6. Standing, M.B.: "Inflow Performance Relationships for Damaged Wells Producing by Solution-Gas Drive," J.Pet.Tech. (Nov., 1970) 1399-1400.

7. Standing, M.B.: "Concerning the Calculation of Inflow Performance of Wells Producing from Solution Gas Drive Reservoirs," J.Pet.Tech. (Sept., 1971) 1141-1142.

8. Patton, L.D. and Goland, M.: "Generalized IPR Curves For Predicting Well Behavior," Pet.Eng. (Sept., 1980) 92-102.

9. Richardson, J.M. and Shaw, A.H.: "Two-Rate IPR Testing - A Practical Production Tool," J.Can.Pet.Tech. (March-April, 1982) 57-61.

10. Fetkovich, M.J.: "The Isochronal Testing of Oil Wells," paper SPE 4529 presented at the SPE-AIME 48th Annual Fall Meeting, Las Vegas, Nev., Sept.30-Oct.3, 1973.

11. Al-Hussainy, R., Ramey, H.J., Jr., and Crawford, P.B.: "The Flow of Real Gases Through Porous Media," J.Pet.Tech. (May, 1966) 624-636; Trans., AIME, Vol. 237.

12. Earlougher, R.C., Jr.: Advances in Well-Test Analysis, SPE Monograph Series, Vol. 5, Dallas (1977).

13. Theory and Practice of the Testing of Gas Wells, Energy Resources Conservation Board, Calgary, Alberta, Canada, Chapter 4.

14. Raghavan, R.: "Well Test Analysis: Wells Producing by Solution Gas Drive," J.Pet.Tech. (Aug., 1976) 196-208; Trans., AIME, Vol. 261.

15. Boe, A., Skjaeveland, S.M., and Whitson, C.H.: "Two-Phase Pressure Test Analysis," paper SPE 10224 presented at the SPE-AIME 56th Annual Fall Meeting, San Antonio, Tex., Oct. 5-7, 1981.

16. Dias-Couto, L.E. and Golan, M.: "General Inflow Performance Relationship for Solution-Gas Reservoir Wells," J.Pet.Tech. (Feb., 1982) 285-288.

APPENDIX A - DISCUSSION OF STANDING'S METHOD FOR CORRECTING INFLOW PERFORMANCE OF DAMAGED/STIMULATED WELLS

Standing suggests a method for using the Vogel relation to average results of multirate tests and to correct for damage or stimulation in the near-wellbore region. The averaging procedure should probably not be used since valuable data showing rate-dependent skin effects might be lost.

To ease the comparison with Standing's work it is assumed that HVF effects are neglible (D=0) and that dimensionless pseudopressure, m_d, equals the Vogel rate-ratio, q_o/q_{omax}. This assumption, as shown by Fetkovich, may result in erroneous interpretation of test data.

Instead of limiting the discussion to Vogel's relation, equations are developed in terms of the general quadratic form (Eq. 20). Following Standing's arguments, the ratio of rate to AOFP with $E_F = 1$ (no-skin) is

$$q_o/q_{omax}^{E_F=1} = 1 - V(p_{wf}^{E_F=1}/p_R) - (1-V)(p_{wf}^{E_F=1}/p_R)^2, \quad \dots \quad (A-1)$$

The no-skin wellbore flowing pressure, $p_{wf}^{E_F=1}$, is given by

$$p_{wf}^{E_F=1} = p_{wf} + \Delta p_s. \quad \dots\dots\dots\dots\dots\dots\dots\dots\dots\dots\dots \quad (A-2)$$

where p_{wf} is the measured wellbore flowing pressure, and Δp_s is pressure drop due to skin - positive for positive skin and negative for negative skin.

Using the definition of flow efficiency,

$$E_F = \frac{p_R - p_{wf} - \Delta p_s}{p_R - p_{wf}}, \quad \dots\dots\dots\dots\dots\dots\dots \quad (A\text{-}3)$$

the no-skin wellbore flowing pressure is given by

$$p_{wf}^{E_F=1} = p_{wf} \cdot E_F + (1-E_F) \cdot p_R. \quad \dots\dots\dots\dots\dots \quad (A\text{-}4)$$

Standing suggests that E_F be estimated by

$$E_F \approx \frac{\ln(r_e/r_w)-3/4}{\ln(r_e/r_w)-3/4+s}. \quad \dots\dots\dots\dots\dots\dots \quad (A\text{-}5)$$

To arrive at this expression the oil pressure function, $F(p)$, must be approximately the same at average pressure and in the skin zone. It also assumes that pressure drop in the reservoir is given by

$$q_o = \frac{2\pi akh}{\ln(r_e/r_w)-3/4} \cdot \frac{k_{ro}}{\mu_o B_o} \cdot (p_R - p_{wf}^{E_F=1}), \quad \dots\dots\dots\dots \quad (A\text{-}6)$$

If $k_{ro}/\mu_o B_o$ is evaluated at the average of p_R and $p_{wf}^{E_F=1}$, then Eq. A-6 is consistent with the Vogel relation. The pressure function in the near-wellbore region is probably less than tzis value. A more correct expression for E_F is given by

$$E_F = \frac{\ln(r_e/r_w)-3/4}{\ln(r_e/r_w)-3/4 + s \cdot F(p_{avg})/F(p_{skin})} . \quad \text{....... (A-7)}$$

The ratio $F(p_{avg})/F(p_{skin})$ can be shown to equal

$$\frac{F(p_{avg})}{F(p_{skin})} = \frac{2x + (1-x)\{2+E_F(p_{wf}/p_R-1)\}/2}{2x + (1-x)\{1-E_F+(1+E_F)p_{wf}/p_R\}/2}, \quad \text{... (A-8)}$$

which can be simplified by evaluating the pressure function in the near-wellbore region at the measured wellbore flowing pressure, p_{wf},

$$\frac{F(p_{avg})}{F(p_{skin})} \simeq \frac{2x + (1-x)(1+p_{wf}/p_R)/2}{2x + (1-x) \cdot p_{wf}/p_R} . \quad \text{............ (A-9)}$$

Fig. A-1 shows the influence of the pressure-function ratio on flow efficiency for several values of positive skin; $\ln(r_e/r_w)-3/4$ equal to 7 and Vogel's pressure function ($x=1/9$) are used. The influence is greatest at large drawdowns (low p_{wf}/p_R values) and skin less than 10. The approximation given by Eq. A-9 is good at p_{wf}/p_R above 0.5 but is relatively large for large drawdowns with skin values of 3 to 5. The correction should not be applied to wells with negative skin factors.

Using the Standing procedure for stimulated wells can lead to nonphysical results. Fig. A-2 shows the case of a well with E_F of 1.5 (highly stimulated). The no-skin wellbore flowing pressure is <u>negative</u> at measured wellbore flowing pressures less than $p_R(E_F-1)/E_F$; one-third p_R for E_F of 1.5. Also, at measured wellbore flowing pressures less than

$p_R \cdot \{(E_F-1-x/(1-x)/E_F\}$ the rate <u>decreases</u> with increasing drawdown; at one-fourth p_R for E_F of 1.5 using Vogel's relation.

Assuming an estimate of E_F can be made, the general rate-pressure relation using Standing's arguments is

$$q_o/q_{omax}^{E_F=1} = 1 - V\{(p_{wf}/p_R)E_F + (1-E_F)\}$$
$$- (1-V)\{(p_{wf}/p_R)E_F + (1-E_F)\}^2, \quad \ldots\ldots (A-10)$$

or

$$q_o/q_{omax}^{E_F \neq 1} = \frac{q_o/q_{omax}^{E_F=1}}{1 - V(1-E_F) - (1-V)(1-E_F)^2}. \quad \ldots\ldots (A-11)$$

The denominator in Eq. A-11 represents the ratio of AOFP with skin to AOFP without skin. Eq. A-10 reproduces Standing's Fig. 2 for V of 0.2 (x of 1/9); an equivalent expression is given by Couto and Golan[16] for V of 0.2.

TABLE 1 - UNITS CONVERSION FACTORS

Quantity	Field		SPE Preferred SI	
	Gas	Oil	Gas	Oil
a	0.006328	0.001127	$8.527 \cdot 10^{-8}$	
a_t	0.0002637		$3.553 \cdot 10^{-9}$	
a_{HVF}	$3.061 \cdot 10^{6}$	634.5	$9.326 \cdot 10^{8}$	$1.085 \cdot 10^{6}$
k	md		md ($\simeq \mu m^2$)	
h	ft		m	
r	ft		m	
p	psia		kPa	
c	1/psi		1/kPa	
μ	cp		Pa·s	
γ	air=1	water=1	air=1	water=1

TABLE 2 - ROCK AND FLUID PROPERTIES FOR VOGEL DATA

	Read From Vogel's Fig. 9a					Evinger-Muskat Method Using R of 102.4 Sm³/Sm³					
p	R_s	B_o	$\mu_o \cdot 10^3$	$B_g \cdot 10^3$	$\mu_g \cdot 10^3$	k_{rg}/k_{ro}	k_{ro}	$F(p)$	$\Delta m \cdot 10^{-3}$	$m(p) \cdot 10^{-3}$	m_d
(kPa)	(Sm³/Sm³)	(m³/Sm³)	(Pa·s)	(m³/Sm³)	(Pa·s)	(Eq.22)	(below)	(1/Pa·s)	(kP/Pa·s)		
14686	102.4	1.30	1.03	6.67	0.0195	0.0	0.444	331.6	276.8 a	2553.1	0.000
13790	98.85	1.29	1.04	7.13	0.0188	0.000356	0.384	286.1	469.8	2276.3	0.108
12066	93.51	1.28	1.12	8.08	0.0178	0.000893	0.371	259.1	419.8	1806.5	0.292
10342	85.49	1.27	1.22	9.46	0.0169	0.00174	0.353	228.0	361.8	1386.7	0.457
8618	75.70	1.26	1.38	11.4	0.0159	0.00278	0.334	191.8	306.0	1024.9	0.598
6895	66.79	1.25	1.60	14.1	0.0152	0.00382	0.326	163.3	257.6	718.9	0.718
5171	56.99	1.23	1.93	19.4	0.0142	0.00527	0.322	135.6	210.2	461.3	0.819
3447	44.53	1.18	2.47	27.7	0.0134	0.00737	0.316	108.3	161.4	251.1	0.902
1724	30.28	1.14	3.30	58.8	0.0124	0.0140	0.297	79.0	88.2	89.7	0.965
101	0.00	1.02	4.23	1000.0	0.0114	0.270	0.128	29.7	1.5	1.5	0.999

a. $276.8 \cdot 10^3 = (14686-13790)(331.6+286.1)/2.$ $m(p) = \Delta m$ starting at atmospheric pressure (101 kPa).

Read From Vogel's Fig. 10a

S_o	k_{ro}	k_{rg}
0.806	0.444	0.0
0.781	0.390	0.000039
0.756	0.329	0.001
0.706	0.238	0.01
0.656	0.159	0.023
0.606	0.096	0.047
0.556	0.052	0.078
0.506	0.026	0.115

TABLE 3 - RESERVOIR ROCK AND FLUID PROPERTIES FOR GAS WELL IN EXAMPLE 1

Numerical Model:

1-Dimensional, Radial, Fully-Explicit (Fully-Implicit Check)
40 Blocks with Radii at Pressure Points $r_j = 1.252 \cdot r_{j-1}$ ($r_1 = 0.1006$ m).
Minimum:Maximum Time Step (days) $= 10^{-11} : 0.1$ with Multiplication
Factor 1.5.

General Properties:

r_w	$= 0.1006$ m	p_i	$= 20684$ kPa
r_e	$= 642.1$ m (320 acre)	T	$= 79.44$ °C
h	$= 30.48$ m	γ_g	$= 0.75$ (air=1)
k	$= 0.01$ md ($\approx \mu m^2$)	S_g	$= 1.0$
ϕ	$= 0.1$	c_{gi}	$= 4.1047 \cdot 10^{-8}$ kPa^{-1}
β	$= 3.936 \cdot 10^{15}$ m^{-1}	B_{gi}	$= 4.9240 \cdot 10^{-4}$ m^3/Sm^3

p (kPa)	$\mu_g \cdot 10^3$ (Pa·s)	Z	$p/\mu_g Z \cdot 10^{-6}$ (kPa/Pa·s)	$\Delta m \cdot 10^{-12}$ (kPa^2/Pa·s)	$m(p) \cdot 10^{-12}$
22408	0.02280	0.8347	1177	2.015 [a]	33.756
20684	0.02167	0.8229	1160	1.977	29.726
18961	0.02054	0.8149	1134	1.922	25.772
17237	0.01942	0.8091	1097	1.847	21.928
15513	0.01834	0.8084	1046	1.747	18.234
13790	0.01730	0.8127	981	1.620	14.740
12066	0.01630	0.8222	899	1.463	11.500
10342	0.01546	0.8370	799	1.279	8.574
8618	0.01469	0.8566	685	1.071	6.016
6895	0.01403	0.8805	558	0.845	3.874
5171	0.01348	0.9075	423	0.608	2.184
3447	0.01304	0.9369	282	0.364	0.968
1724	0.01271	0.9679	140	0.120	0.240
101	0.01252	0.9981	8	0.000	0.000

a. $2.015 \cdot 10^{12} = (22408-20684)(1177+1160) \cdot 10^6/2$

TABLE 4 - TEST PROGRAM AND RESULTS FOR GAS WELL IN EXAMPLE 1

t (hr)	Δt (hr)	q_g (Sm³/d)	p_w (kPa)	$m(p_w)\cdot10^{-12}$ (kPa²/Pa·s)	m_d
-	-	-	20684	29.73	-
0- 12	12	1413	16058	22.78	-
12- 36	24	0	20484	29.27	-
36-180	144	0	20652	29.65	-
180-188	8	565	19257	26.45	0.108
188-196	8	0	20517	29.35	-
196-204	8	1130	17322	22.12	0.246
204-212	8	0	20320	28.89	-
212-220	8	1696	14715	16.62	0.425
220-228	8	0	20080	28.34	-
228-236	8	2261	10928	9.57	0.662
236-242	8	0	19797	27.70	-
242-250	8	2826	2082	0.39	0.986 [a]
250-274	24	0	20322	28.90	-

a. Highest rate not used to analyze data.

TABLE 5 - AOFP CORRECTION FOR GAS WELL IN EXAMPLE 1

t (yr)	t_D	p_D [a]	New AOFP (Sm³/d)[b]
test	0.00050	3.23	3109
1	0.542	1.16	7593
2	1.08	1.50	5872
5	2.71	1.90	4635
10	5.40	2.22	3967
25	13.6	2.80	3145

a. Uniform-flux solution except for test point. t_{Dpss} for x_e/x_f of 15 is greater than 100.

b. $AOFP_{new} = (3.23-0.4)\times3109/p_D$; -0.4 is steady-state skin estimated from test.

TABLE 6 - ROCK AND FLUID PROPERTIES FOR OILWELL TESTS IN EXAMPLE 2

General Properties:

r_w = 0.1006 m p_i = 25476 kPa (bubble point)

r_e = 1284.2 m (assumed)   T = 93.33 °C

h = 6.096 m γ_{API} = 43.7 °

k = 2470 md ($\approx \mu m^2$) S_{iw} = 0.32

ϕ = 0.21 c_{ti} = $3.626 \cdot 10^{-6}$ kPa^{-1}

Relative Permeability:

Corey Relation (Fig. 8) with λ of 1.

$$k_{ro} = S_o*^5 \qquad k_{rg} = \{1-S_o*\}^2 \cdot \{1-S_o*^{1.5}\} \qquad S_o* = S_o/(1-S_{iw})$$

PVT Properties:

p (kPa)	R_s (Sm³/Sm³)	B_o (m³/Sm³)	$\mu_o \cdot 10^3$ (Pa·s)	$B_g \cdot 10^3$ (m³/Sm³)	$\mu_g \cdot 10^3$ (Pa·s)	$m(p) \cdot 10^{-6}$a (kPa/Pa·s)	R b (Sm³/Sm³)	$\frac{F\{p_R\}}{F\{p_b\}}$
31026	249.3	1.7116	0.2646	3.79	0.0313	32.271	249.3	0.942
29303	249.3	1.7186	0.2583	3.91	0.0301	28.427	249.3	0.961
27579	249.3	1.7265	0.2524	4.05	0.0288	24.508	249.3	0.979
25476	249.3	1.7377	0.2456	4.27	0.0273	19.631	249.3	1.000
24821	241.7	1.7175	0.2493	4.34	0.0268	18.354	241.8	0.933
24132	233.9	1.6962	0.2533	4.43	0.0263	17.335	234.6	0.838
23442	225.8	1.6751	0.2575	4.52	0.0257	16.405	229.0	0.747
22408	214.1	1.6436	0.2641	4.67	0.0249	15.113	227.4	0.624
20684	194.7	1.5918	0.2762	4.98	0.0236	13.144	264.3	0.450
17237	156.7	1.4906	0.3054	5.84	0.0208	9.685	661.0	0.241
13790	120.4	1.3931	0.3442	7.32	0.0182	6.722	1719.0	0.139
10342	85.5	1.3001	0.3993	10.1	0.0160	4.210	3526.0	0.083
6895	52.9	1.2129	0.4849	16.1	0.0143	2.182		
5171	37.6	1.1720	0.5492	22.3	0.0136	1.367		
3447	23.2	1.1337	0.6401	34.7	0.0131	0.706		
1724	10.2	1.0989	0.7778	71.9	0.0128	0.222		
101	0.4	1.0727	0.9699	124.0	0.0125	0.002		

a. m(p) calculated using the Evinger-Muskat method with R of 249.3 Sm³/Sm³.
b. R and F(p_R) from Tarner material balance.

TABLE 7 - 4-HOUR ISOCHRONAL TEST RESULTS FOR OIL WELL IN EXAMPLE 2.

$m(p_R) \cdot 10^{-6}$ in kPa/Pa·s

	p_R=25476 kPa		19.631 (Evinger-Muskat)		29.847 (Fetkovich)	
Flow ID	q_o (Sm^3/d)	p_{wf} (kPa)	$m(p_{wf}) \cdot 10^{-6}$ (kPa/Pa·s)	m_d	$m(p_{wf}) \cdot 10^{-6}$ (kPa/Pa·s)	m_d
A-1	366.9	24401	17.733	0.0967	27.380	0.0827
A-2	230.8	24950	18.606	0.0522	28.628	0.0409
A-3	120.4	25325	19.336	0.0150	29.494	0.0118
A-4	66.6	25376	19.436	0.0099	29.614	0.0078

$m(p_R) \cdot 10^{-6}$ in kPa/Pa·s

	p_R=24821 kPa		19.070 (Evinger-Muskat)		27.076 (Fetkovich)	
B-1	106.4	24676	18.805	0.0139	26.761	0.0160
B-2	164.6	24475	18.435	0.0333	26.236	0.0277
B-3	224.6	24327	18.165	0.0475	26.009	0.0394
B-4	366.1	23757	17.256	0.0952	24.803	0.0839

a. Test A run 71/12/23 and Test B run 72/06/10.
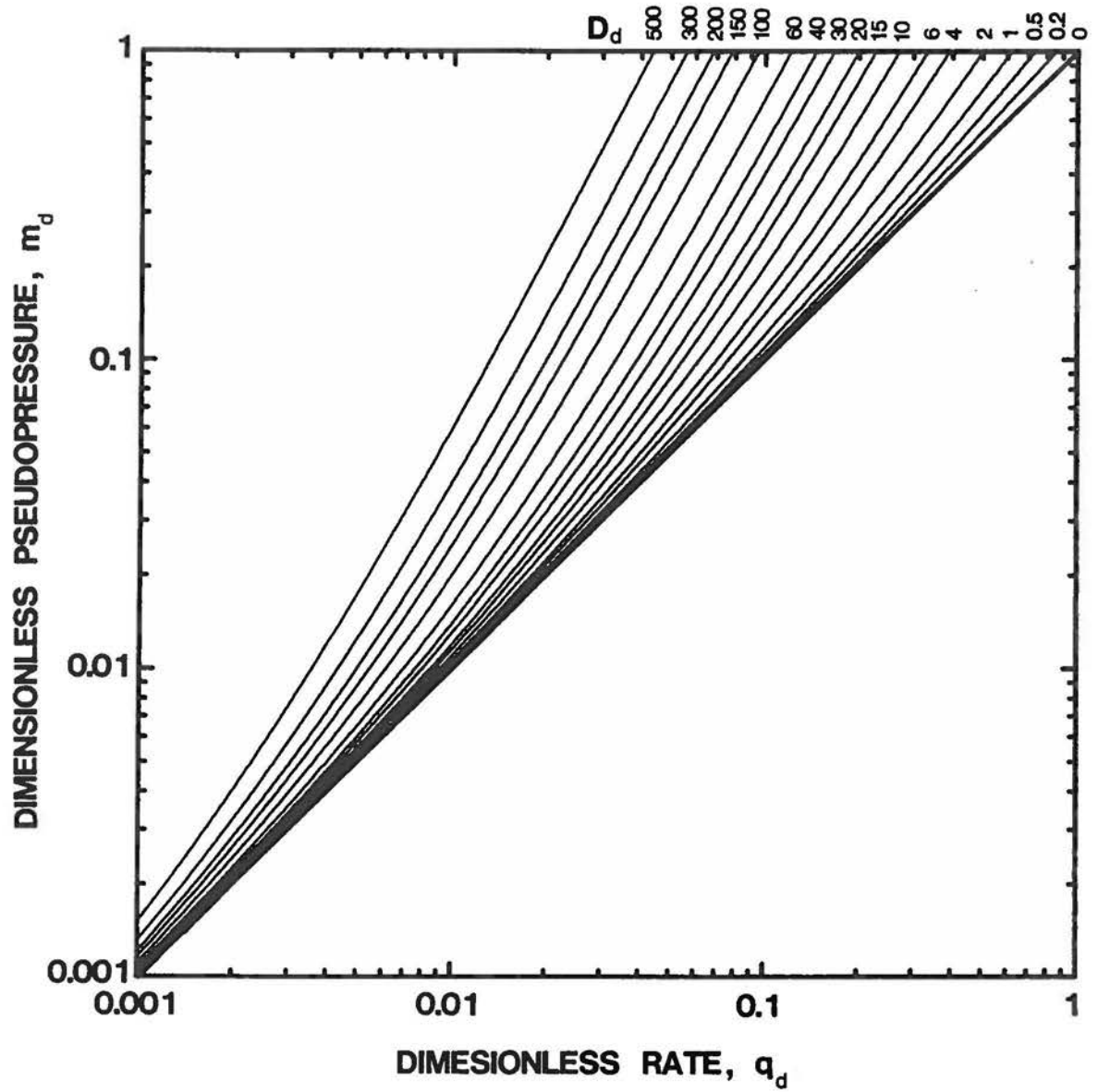
Fig. 1 - Log-log plot of dimensionless rate-pseudopressure solution
including high-velocity-flow effects.
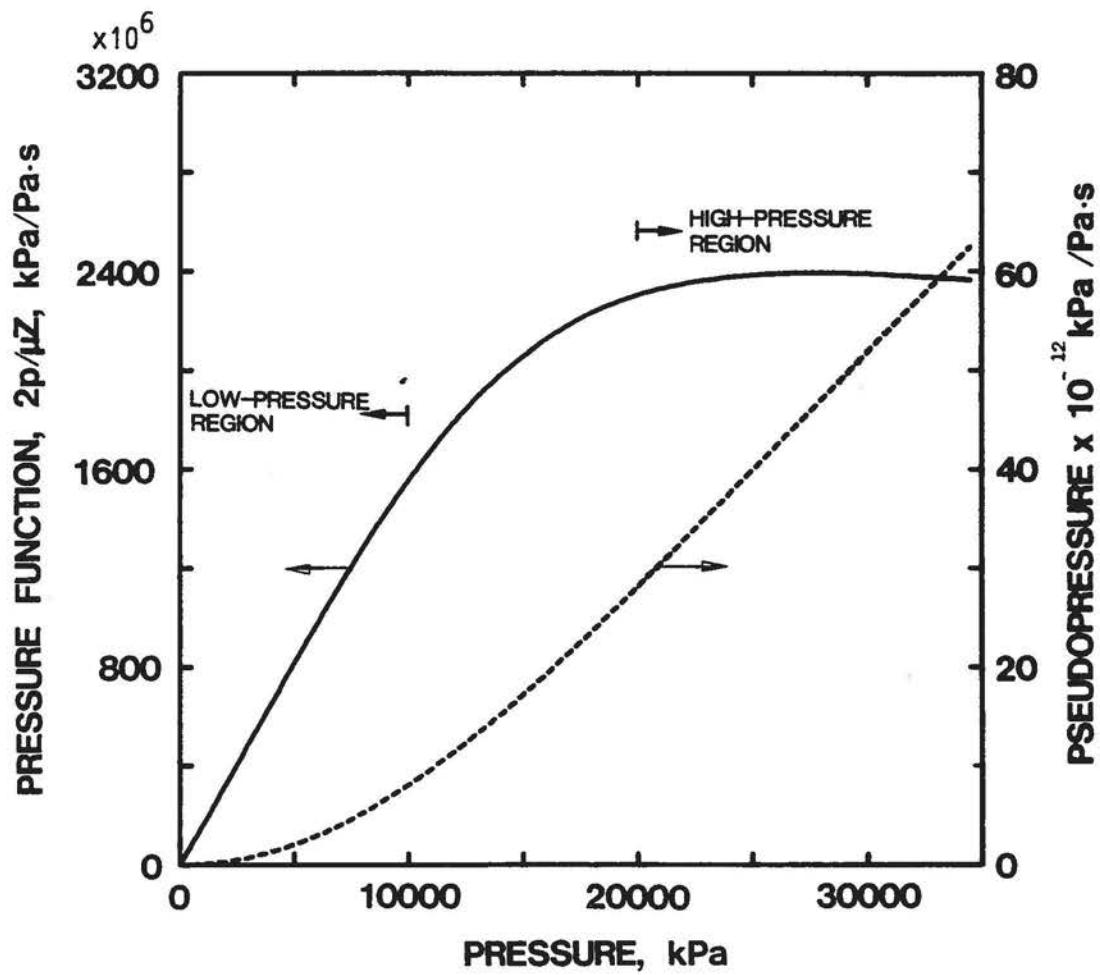
Fig. 2 - Real gas pressure and pseudopressure functions for reservoir
fluid in Example 1.
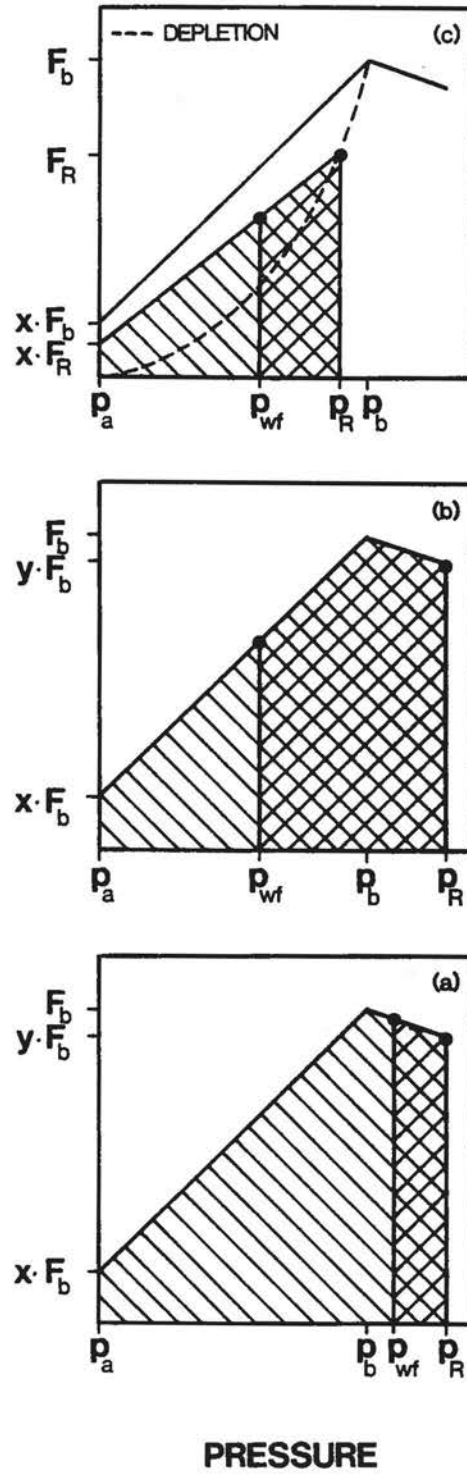
Fig. 3 - Schematic of simplified oil pressure
function for three conditions of flow.
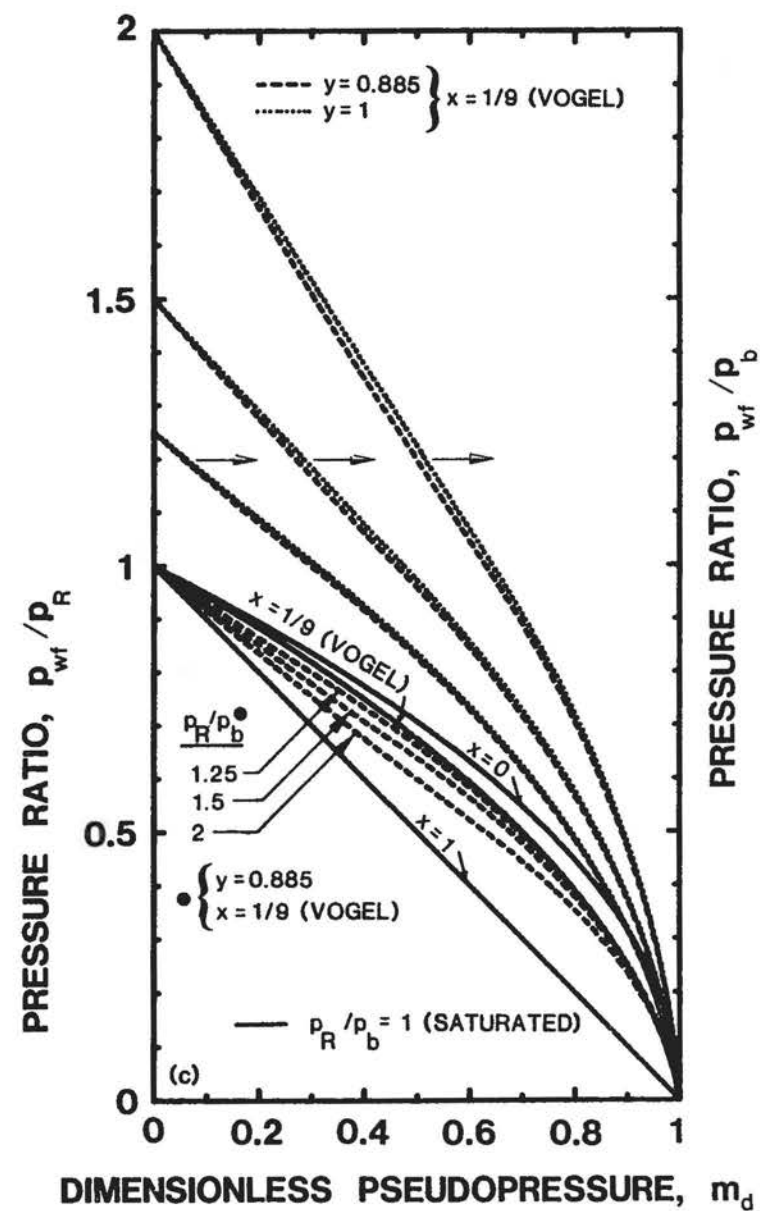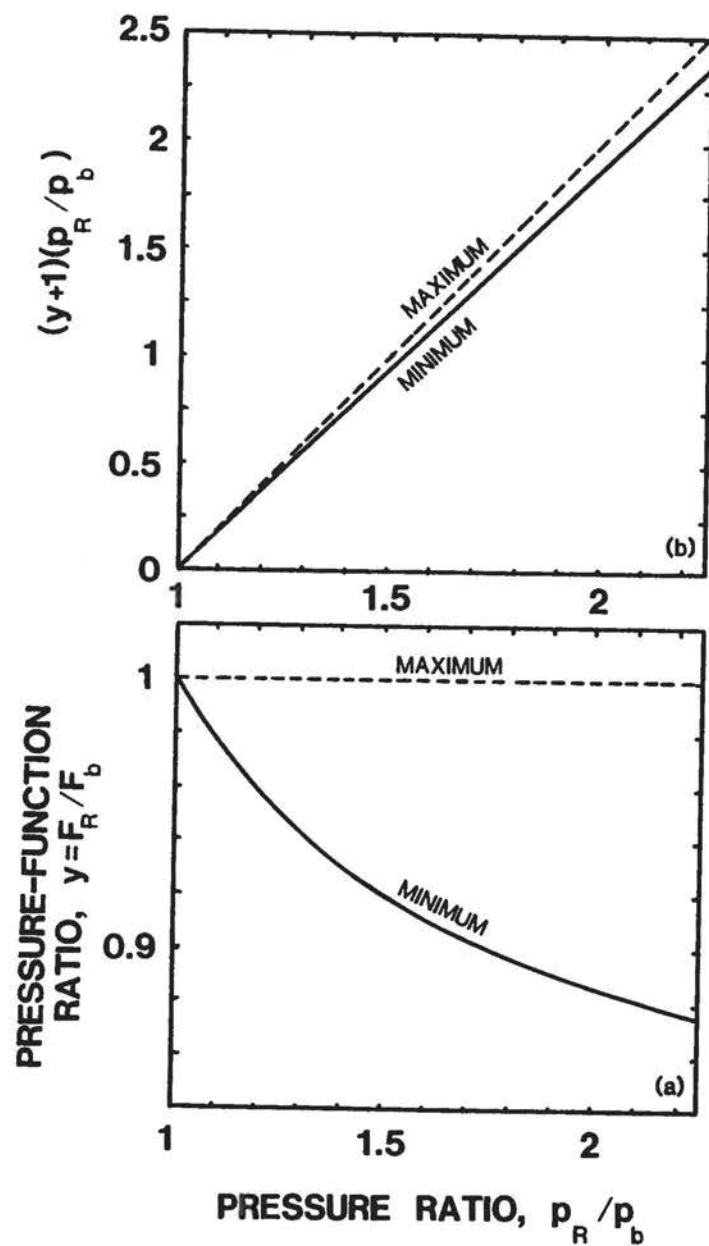
Fig. 4 - Various pressure functions illustrating the effect of undersaturated oil flow on traditional solution-gas drive (saturated) inflow performance.
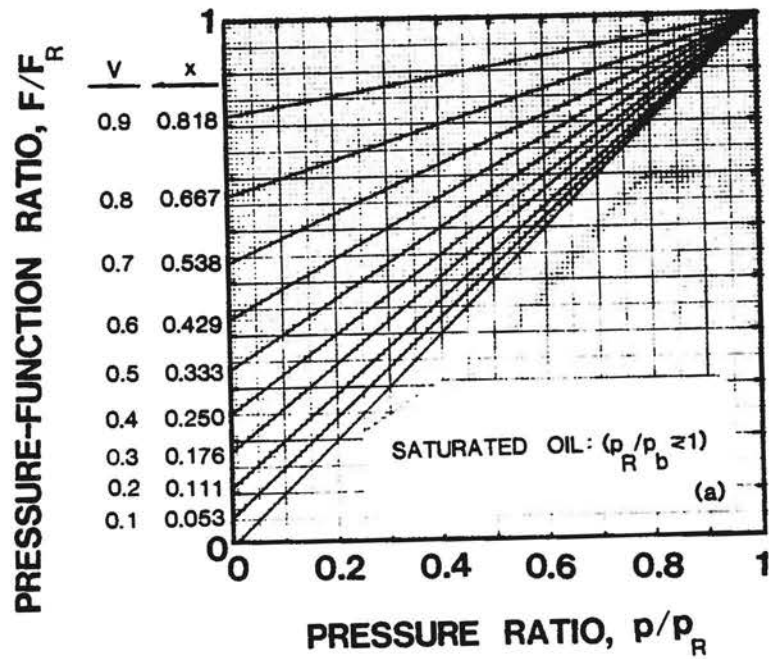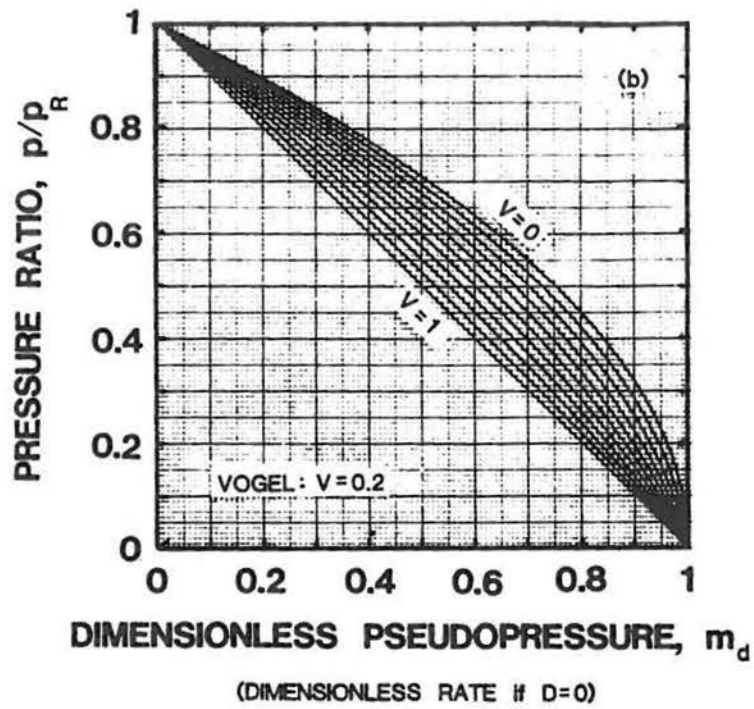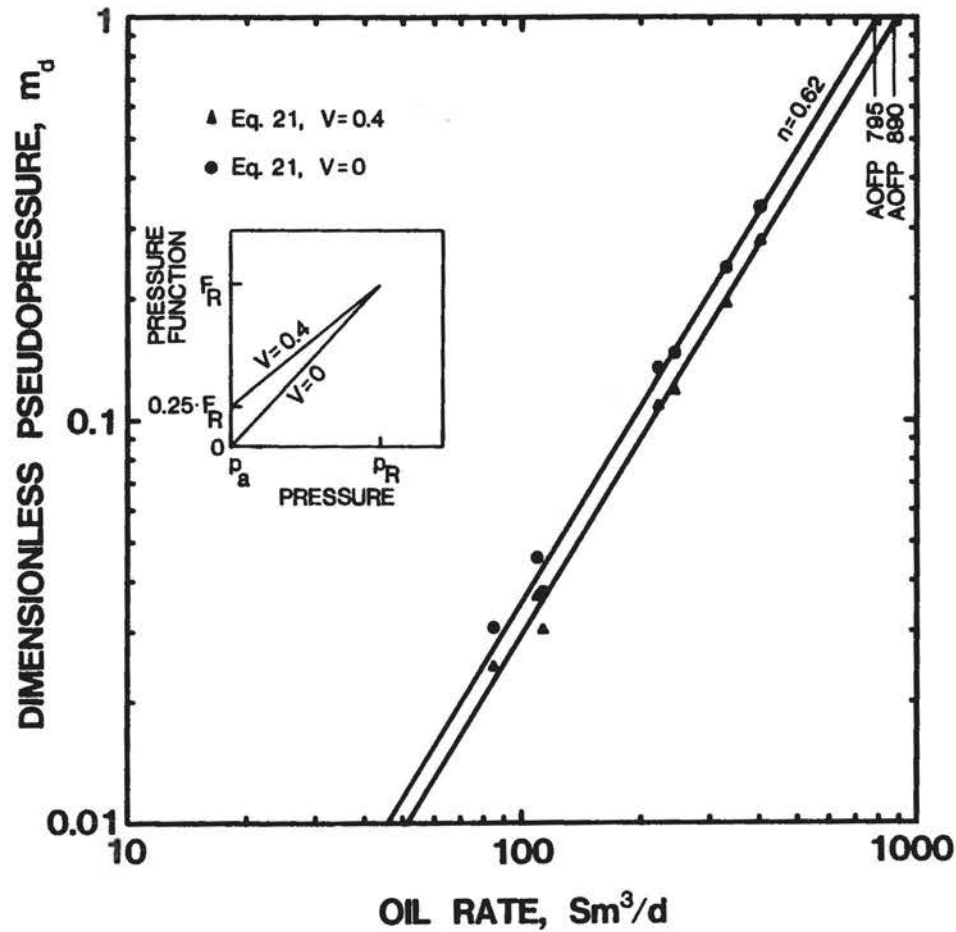
Fig. 5 - Saturated oil pressure and pseudopressure functions.

Fig. 6 - Multirate oilwell test analysed using two
pseudopressure functions (Fetkovich[10] Well 3-C,
Field C).
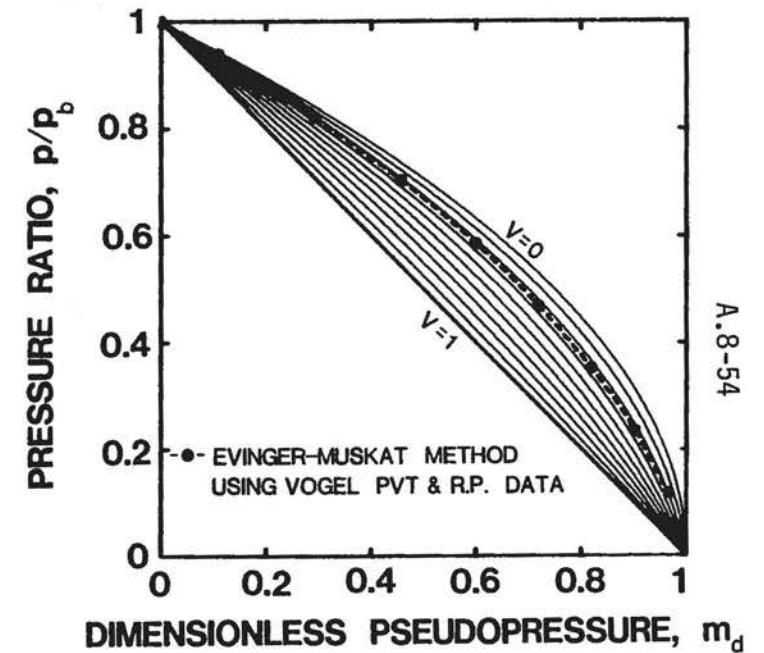
Fig. 7 - Best-fit of pseudopressure function
(dimensionless Vogel rate) using the
Evinger-Muskat method and Vogel's base-
case reservoir rock and fluid data.

A.8-54
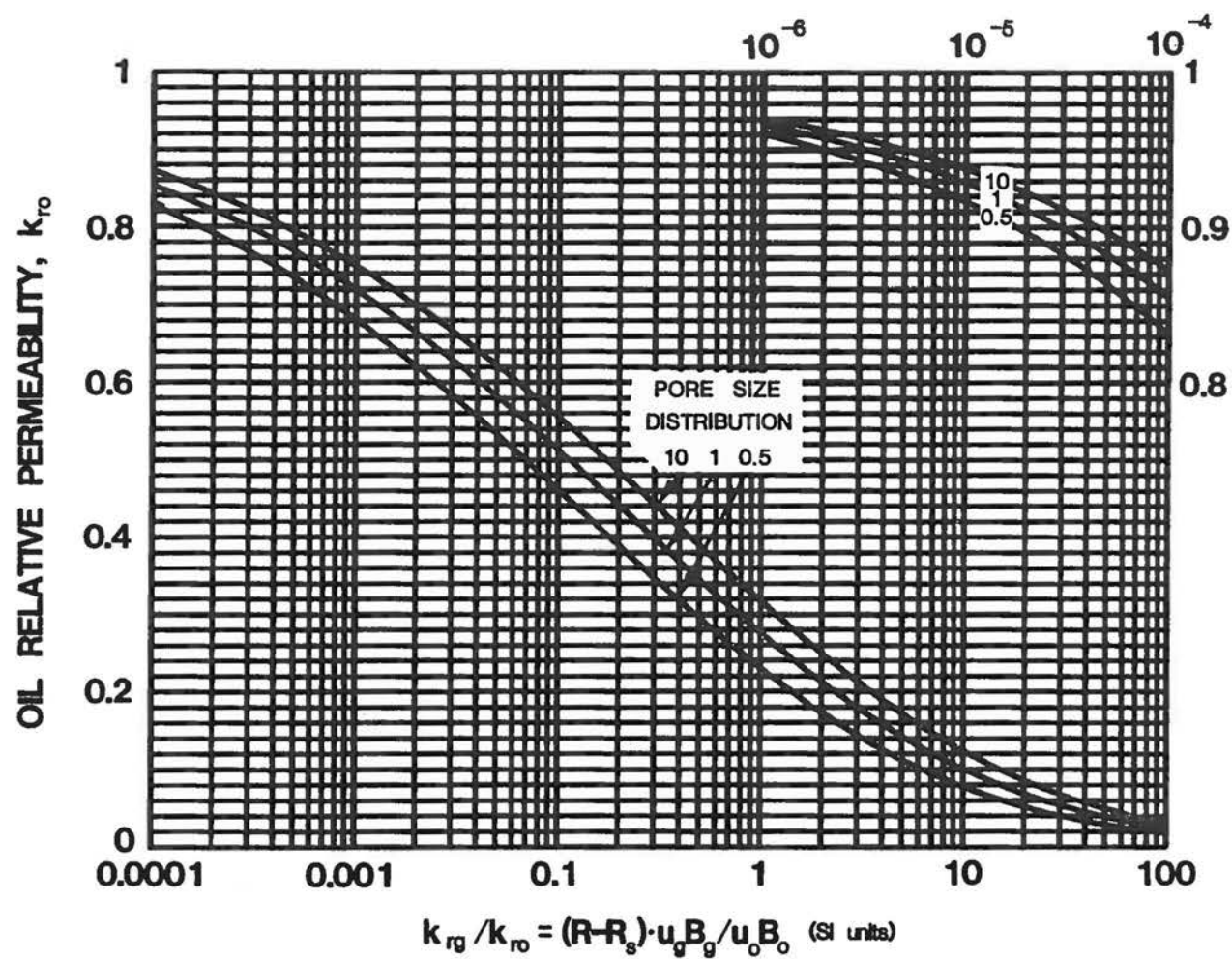
Fig. 8 - Generalized relative permeability relation for use with the Evinger-
Muskat method of calculating saturated oil pseudopressure.
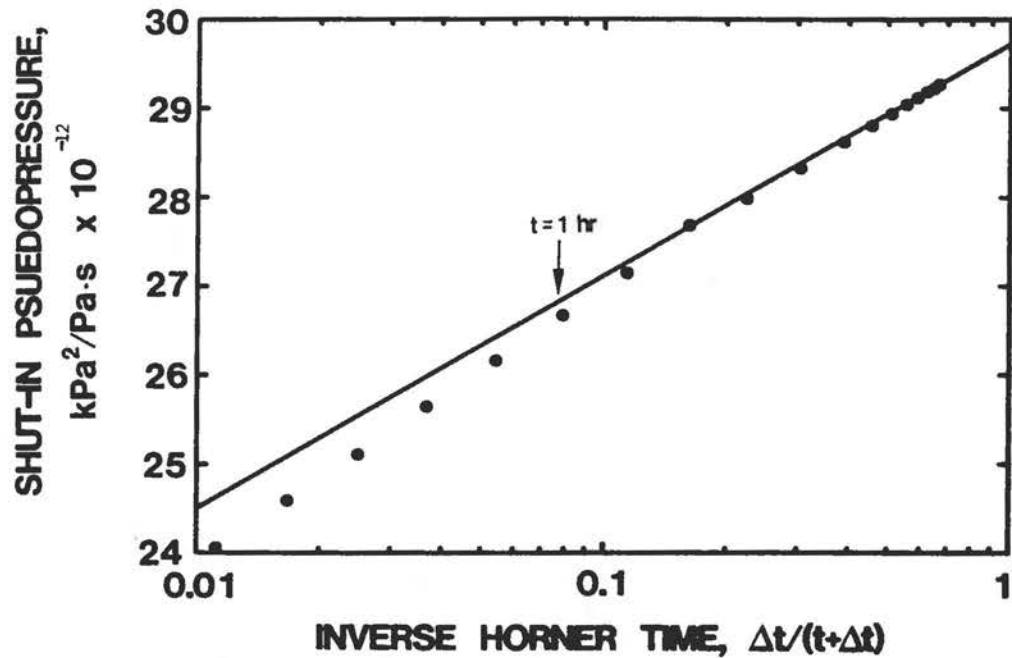
Fig. 9 - Horner analysis of simulated buildup well test in Example 1.
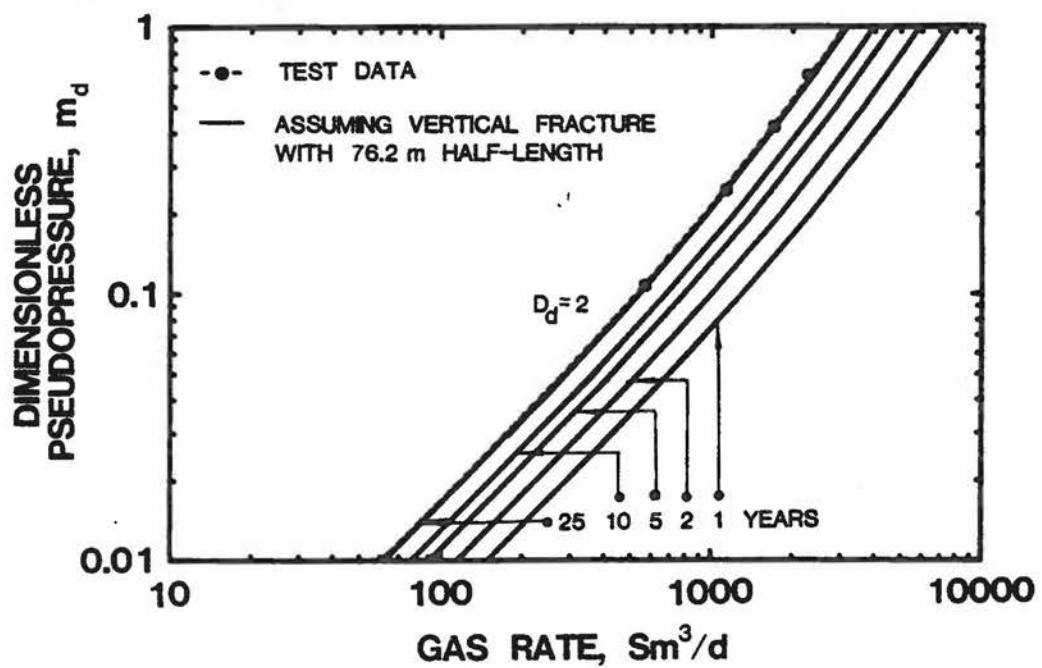
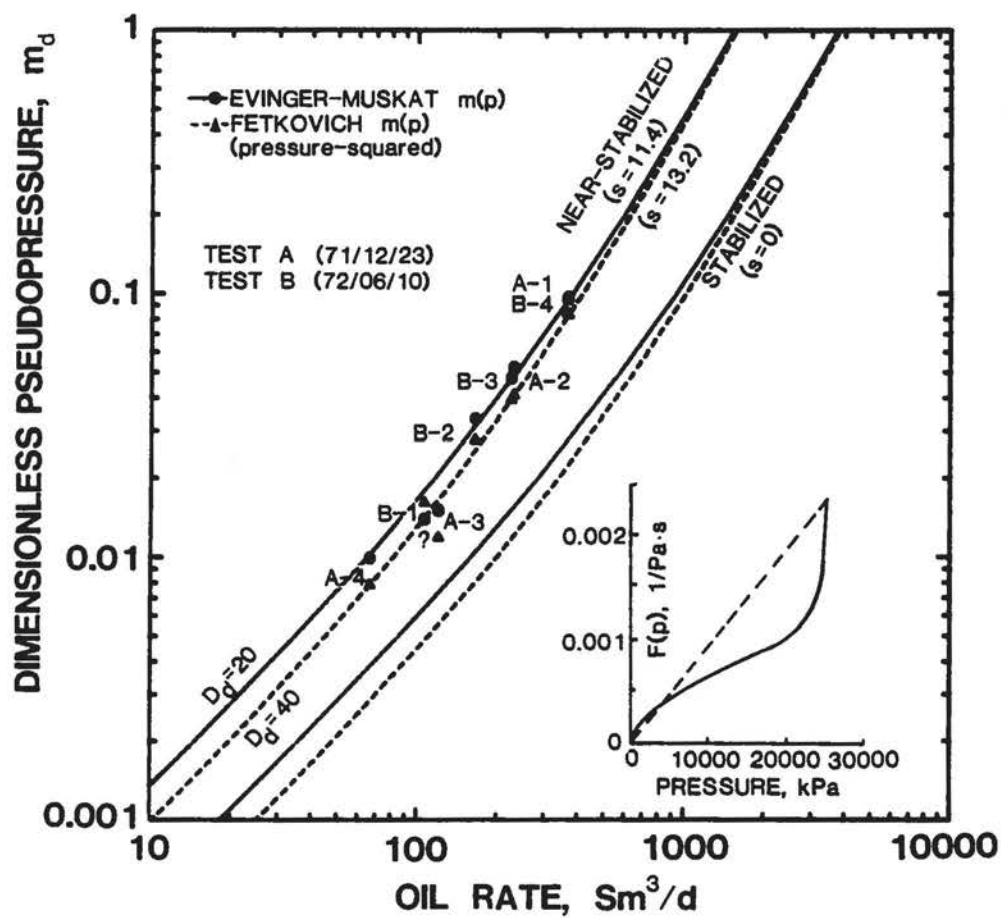Fig. 10 - Log-log type-curve match of gaswell modified isochronal test in Example 1.

Fig. 11 - Log-log type-curve match of oilwell isochronal test in Example 2 (Fetkovich Well 5-C, Field D); insert illustrates saturated oil pressure functions corresponding to the two methods of calculating pseudopressures (Evinger-Muskat vs. Fetkovich).
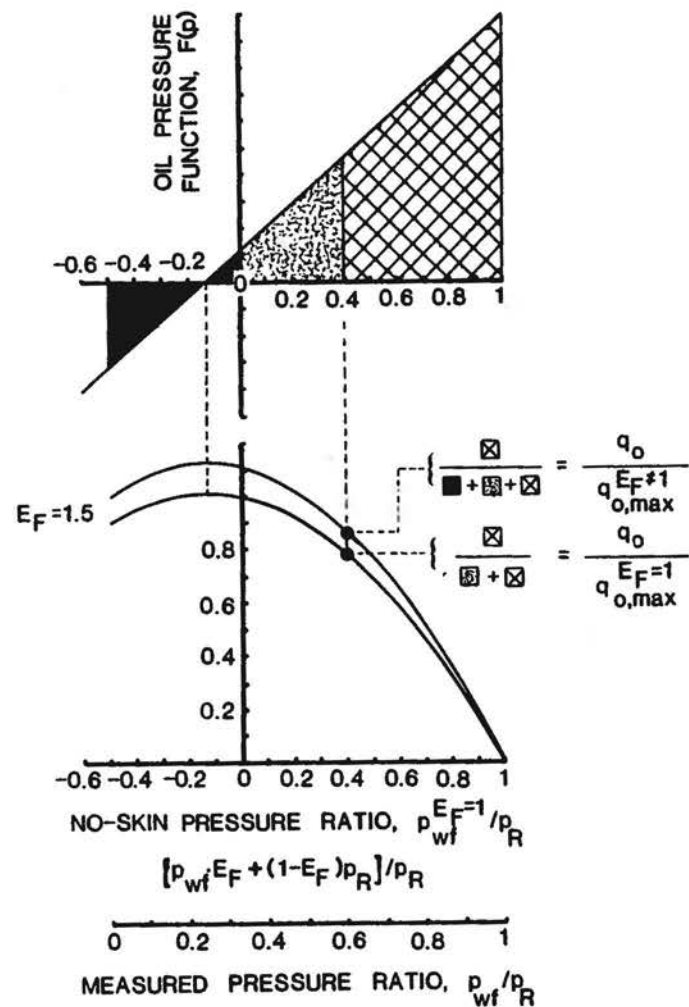
Fig. A-1 - Physical description of why the Standing method for correcting the Vogel relation for stimulated wells can lead to nonphysical rate-pressure behavior.
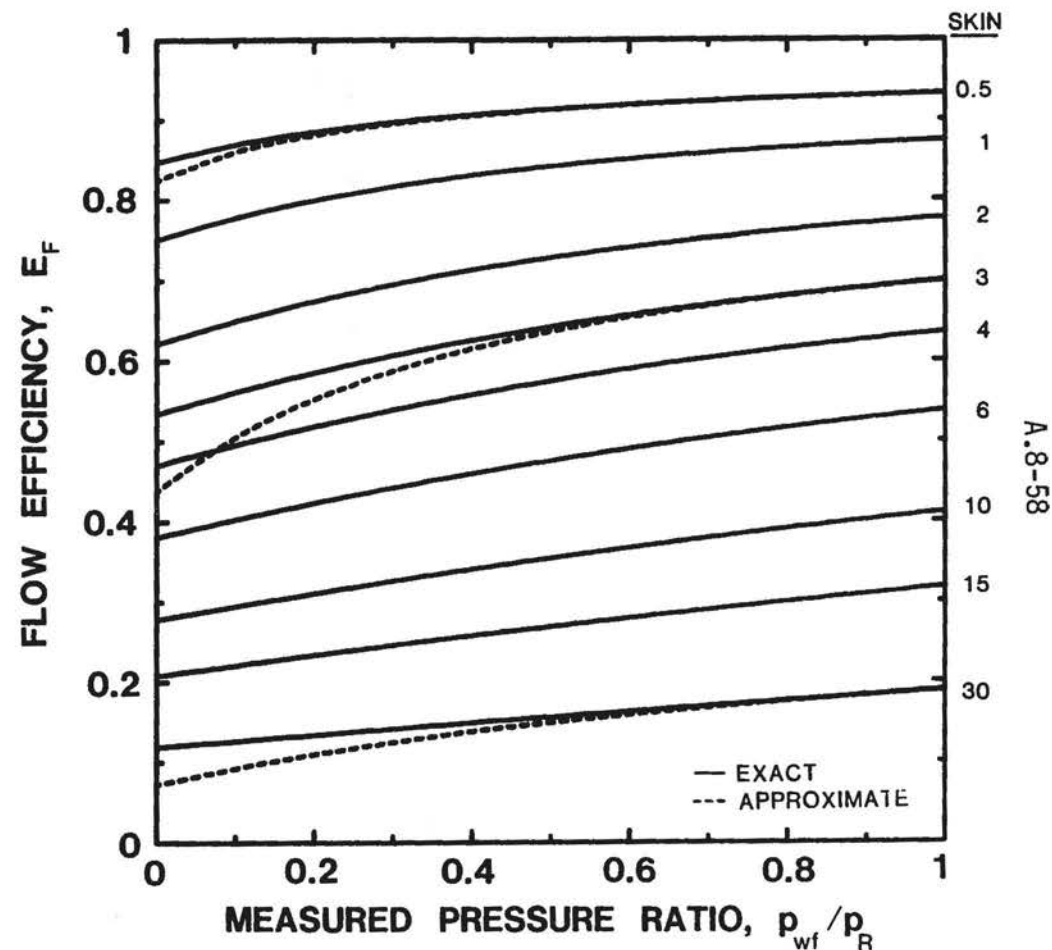
Fig. A-2 - Effect of two-phase, gas-oil flow on the relation between flow efficiency and positive skin factor; $\ln(r_e/r_w)-3/4 = 7$ and Vogel's saturated oil pressure function are assumed.